Design, Synthesis and Biological Evaluation of Covalent Inhibitor of Epidermal Growth Factor Receptor (EGFR) Kinase

NICHAREE JIRACHEEP

A THESIS SUBMITTED IN PARTIAL FULFILLMENT

OF THE REQUIMENTS FOR DEGREE OF

MASTER OF ENGINEERING IN BIOMEDICAL ENGINEERING

FACULTY OF ENGINEERING

KING MONGKUT'S INSTITUTE OF TECHNOLOGY LADKRABANG

2019

KMITL-2019-EN-M-045-097

Design, Synthesis and Biological Evaluation of Covalent Inhibitor of Epidermal Growth Factor Receptor (EGFR) Kinase

NICHAREE JIRACHEEP

A THESIS SUBMITTED IN PARTIAL FULFILLMENT

OF THE REQUIMENTS FOR DEGREE OF

MASTER OF ENGINEERING IN BIOMEDICAL ENGINEERING

FACULTY OF ENGINEERING

KING MONGKUT'S INSTITUTE OF TECHNOLOGY LADKRABANG

2019

KMITL-2019-EN-M-045-097

การศึกษา ออกแบบ และสังเคราะห์ตัวยับยั้งโคเวเลนต์ของโปรตีนไคเนสชนิด EGFR และการทดสอบผลทางชีววิทยา

ณิชารีย์ จิรชีพ

วิทยานิพนธ์นี้เป็นส่วนหนึ่งของการศึกษาตามหลักสูตรปริญญาวิศวกรรมศาสตรมหาบัณฑิต

สาขาวิชาวิศวกรรมชีวการแพทย์

คณะวิศวกรรมศาสตร์

สถาบันเทคโนโลยีพระจอมเกล้าเจ้าคุณทหารลาดกระบัง

2019

KMITL-2019-EN-M-045-097

Table of Contents

page

List of Tables

Table **Page**

List of Schemes

Scheme **Page**

List of Figures

List of Abbreviations

ADC	=	Adenocarcinoma
APCI	=	Atmospheric Pressure Chemical Ionization
ATP	=	Adenosine triphosphate
°C	=	Degree of celsius
Cat.	=	Catalyst
CO_2	=	Carbon dioxide
$(COCl)_2$	=	Oxalyl chloride
CO	=	Carbon monoxide
DCM	=	Dichloromethane
DIPEA	=	N,N-Diisopropylethylamine
DMA	=	Dimethylacetamide
DMEM	=	Dulbecco's Modified Eagle Medium
DMF	=	Dimethylformamide
DMSO	=	Dimethyl sulfoxide
EGFR	=	Epidermal Growth Factor Receptor
Equiv.	=	equivalent
ESI	=	Electrospray ionization
EtOAc	=	Ethyl acetate

List of Abbreviations (cont.)

FBS	=	Fetal Bovine Serum
FTIR	=	Fourier Transform Infrared
GLOBOCAN	=	Global Cancer Incidence, Mortality and Prevalence
HATU	=	1-[Bis(dimethylamino)methylene]-1H-1,2,3-triazolo[4,5-b]pyridinium 3-oxid hexafluorophosphate
HCl	=	Hydrochloric acid
HPLC	=	High Performance Liquid Chromotagraphy
HRMS	=	High Resolution Mass Spectrometer
Hz	=	Hertz
ia	=	inactive compound
IC_{50}	=	The half maximal inhibitory concentration
MAPK	=	Mitogen-Activated Protein Kinase
μM	=	micromolar
M	=	Molar
MeOH	=	Methanol
$MgCl_2$	=	Magnesium chloride
EGTA	=	Egtazic acid
DTT	=	Dithiothreitol

List of Abbreviations (cont.)

mL	=	millilitre
MW	=	Molecular weight
N_2	=	Nitrogen
NMR	=	Nuclear Magnetic Resonance
nM	=	nano molar
Na_2CO_3	=	Sodium carbonate
$NaHCO_3$	=	Sodium bicarbonate
Na_2SO_4	=	Sodium sulfate
NSCLC	=	Non-Small Cell Lung Cancer
PBS	=	phosphate buffer solution
PD	=	Pharmacodynamic
PDB	=	Protein Data Bank
$Pd(PPh_3)_4$	=	Tetrakis(triphenylphosphine)palladium (0)
PI3K	=	Phosphoinositide 3-kinase
PI3K/Akt	=	phosphatidylinositol-3-OH kinase
PK	=	pharmacokinetic
ppm	=	parts per million
RTK	=	Receptor Tyrosine Kinases

List of Abbreviations (cont.)

SAR	=	Structure-Activity Relationships
$SnCl_2$	=	Tin(II) chloride
STAT	=	Signal Transducer And Activator of Transcription
TEA	=	Triethylamine
TFA	=	Trifluoroacetic acid
THF	=	Tetrahydrofuran
TKI	=	Tyrosine Kinase Inhibitor
TLC	=	Thin Layer Chromatography
USFDA	=	US Food and Drug Administration

หัวข้อวิทยานิพนธ์ การศึกษา ออกแบบ และสังเคราะห์ตัวยับยั้งโคเวเลนต์ของโปรตีนไคเนสชนิด EGFR และการทดสอบผลทางชีววิทยา

นักศึกษา นางสาวณิชารีย์ จิรชีพ

รหัสประจำตัว 59601120

ปริญญา วิศวกรรมศาสตรมหาบัณฑิต

สาขาวิชา วิศวกรรมชีวการแพทย์

พ.ศ. 2562

อาจารย์ที่ปรึกษาวิทยานิพนธ์ รศ.ดร.แมทธิว พอล กลีสัน

อาจารย์ที่ปรึกษาวิทยานิพนธ์ร่วม ดร.กนกทิพย์ บุญยรัตกลิน

บทคัดย่อ

Epidermal growth factor receptors (EGFR) เป็นโปรตีนไคเนสที่มีปัจจัยสำคัญต่อการเกิดและเติบโตของเซลล์มะเร็งปอดชนิด non-small cell lung cancer (NSCLC) ซึ่งในงานวิจัยนี้จะทำการศึกษาและพัฒนาตัวยับยั้งโปรตีนไคเนสโดยที่โครงสร้างหลักเป็นโควาเลนต์ไพริมิดีน รวมไปถึงการศึกษาถึงหมู่ฟังก์ชันของอิเล็กโตรไฟล์ที่สามารถเพิ่มประสิทธิภาพและความจำเพาะเจาะจงต่อโปรตีนไคเนสชนิดนี้ได้ ทั้งนี้สารที่ได้จากการสังเคราะห์จะนำไปทำการวิเคราะห์ทางชีวเคมีกับโปรตีนและทดสอบผลที่เกิดขึ้นทางชีวภาพ (in vitro assay) เพื่อสามารถเข้าใจในประสิทธิภาพของสารเทียบเท่ากับยารักษาจริง ยิ่งไปกว่านั้นจุดมุ่งหมายเพิ่มเติมในงานวิจัยนี้คือมุ่งหวังที่จะพัฒนาทรัพย์สินทางปัญญาเกี่ยวของกับตัวยับยั้งโปรตีนไคเนส รวมไปถึงการกลายพันธุ์ของ EGFR ที่จะสามารถทำให้ทวีปเอเชีย โดยเฉพาะในประเทศไทย สามารถเข้าถึงยารักษาเหล่านี้ได้อย่างมีประสิทธิภาพในราคาที่สามารถรักษากันได้อย่างทั่วถึง

Thesis	DESIGN, SYNTHESIS AND BIOLOGICAL EVALUATION OF COVALENT INHIBITOR OF EPIDERMAL GROWTH FACTOR RECEPTOR (EGFR) KINASE
Student	Ms. Nicharee Jiracheep
Student ID.	59601120
Degree	Master of Engineering
Program	Biomedical Engineering
Year	2019
Thesis Advisor	Assoc.Prof. Dr. Matthew Paul Gleeson
Thesis co-advisor	Dr. Kanokthip Boonyarattanakalin

Abstract

Epidermal growth factor receptors (EGFRs) are a large family of tyrosine kinases implicated in the uncontrolled growth of non-small cell lung cancer (NSCLC). In this work, we report the initial results related to the preparation and testing of novel covalent pyrimidine-based EGFR inhibitors. Compounds have been prepared using Pd-catalysed Suzuki coupling reactions of aryl boronic acids at the 2-position of 2,4-dichloropyrimidine followed by the acid-catalysed substitution of anilino reagents at the 2-position. A Michael acceptor group was included at the 4-position of compounds as part of our initial development efforts. We have evaluated compounds in an EGFR kinase biochemical assays and *in-vitro* cell lines (A431) to determine their potential as therapeutic agents. The compound was then compared to known EGFR drugs Erlotinib® and Afatinib®. Molecular modelling has been used to predict the most probable binding mode within the ATP binding site. Our chemotype is predicted to form a covalent adduct between Cysteine 797 and the inhibitor Michael acceptor moiety. The goal of this work is to better understand how these suicidal inhibitors function, and therefore further improved and how selectivity can be obtained over other kinases. With this preliminary information, the design of cheaper and potentially more selective and more effective inhibitors will be possible.

ACKNOWLEDGEMENTS

I would like to acknowledge and thank all who helped, supported, and funded my thesis at King Mongkut's Institute of Technology Ladkrabang.

Firstly, I express my deepest gratitude to my thesis advisor and mentor Assoc.Prof.Dr. Matthew Paul Gleeson of the Department of Biomedical Engineering at King Mongkut's Institute of Technology Ladkrabang. He generously encouraged, guided, and pushed me to make the most of my research experience. In addition, he went beyond the role of thesis advisor by mentoring me through all the year in graduate school. I would also like to thank Dr. Kanokthip Boonyarattanakalin my co-advisor from College of Nanotechnology, King Mongkut's Institute of Technology Ladkrabang for her loving interest and support during my thesis research.

Secondly, I want to extend my acknowledgements to my fellow students, within MPG group for their friendship, support and sincere interest towards my study during all these years. I wish to express my thanks for introducing me to the world of medicinal chemistry.

Finally, an honorable mention goes to my family for their love and always encourage me to get through hard times. I am very thankful for their genuine support to complete this thesis research.

This work was supported by grants from the Thailand Research Fund (TRF) RSA6180073.

Nicharee Jiracheep

Chapter 1

Introduction

1.1 Statement and significance of the problems

Medicinal chemistry lies at the intersection of chemistry, pharmacology and a diverse range of other biological and technological specialties. These are all required in the process that sees the design, chemical synthesis and industrial development of pharmaceutical agents (drugs) for commercial use. Medicinal chemistry relies heavily on organic, physical, and computational chemistry disciplines with additional emphasis on biological areas such as biochemistry, molecular biology, pharmacognosy and pharmacology, toxicology. A key endeavor of the medicinal chemistry is to develop effective designs and execute cutting edge systems and processes to allow the characterization of the chemical matter. To this end, process design and engineering solutions must be applied to generate and analyze the required data in a systematic fashion. It is the job of the medicinal chemist to derive understanding from the biological activities and properties and derive suitable structure-activity relationships (SAR) to facilitate multiple iteration of the design synthetize, test cycles required. The combination of pharmacological and toxicological testing, with iterative cycles of synthetic chemistry, a candidate drug molecule can be identified for further human trials.[1]

Cancer is a group of diseases characterized by the uncontrolled growth and spread of abnormal cells in the body, resulting in death. In addition to the leading cause of death in economically developed countries and developing countries. This is a major public health problem worldwide. For all sites combined, the cancer incidence rate is 20% higher in men than in women, while the cancer death rate is 40% higher.[2] Lung cancer is currently the leading cause incidence and mortality, with 1.4 million annual deaths worldwide in 2008.[3] The American Cancer Society estimates that in 2014, lung cancer

represented over 25% of all cancer fatalities.[4] In Asia accounts for 60% of the world population and half the global burden of cancer. The incidence of cancer cases is estimated to increase from 6.1 million in 2008 to 10.6 million in 2030, due to ageing and growing populations, lifestyle and socioeconomic changes. The distribution of major cancers in different regions of Asia; lung cancer is which accounts for more deaths each year than breast, prostate, and colon cancer combined.[5]

Chemotherapy slightly prolongs survival among patients with advanced disease, but at the cost of clinically significant adverse effects. Furthermore, Chemotherapeutic treatments currently available on the market are insufficient to deal with the large number of cancer subtypes identified at present. Moreover, their increasingly unaffordability means the specialist treatment and expensive medicines are being kept from the masses.[6]

Non-small cell lung cancer (NSCLC) accounts for a high proportion (85%–90%) in lung cancer.[7] It is acknowledged that more effective treatments strategies are needed to tackle this disease. NSCLC has identified driver mutations that may contribute to early carcinogenesis, including epidermal growth factor receptor (EGFR) mutations.[8] Despite a range of pharmacological therapies being available that target epidermal growth factor receptor kinase (EGFR). In addition, it has been found that disease driven mutations are a major cause treatment failure, particularly in Asian populations. The frequency of EGFR mutations in Asian patients are 47.9% compared to 19.2% for Western patients.[9] Indeed, the Asian populace have a greater need for treatments than their Western counterparts because EGFR mutations occur more frequently. However, these patients do not have access to the same resources and systems available in Western countries (high income countries).[10]

Nowadays, small-molecule kinase inhibitors are being intensively pursued as new anticancer therapeutics. From 2009, approximately 80 inhibitors have been advanced to some stage of clinical evaluation.[11] Kinases are cellular signaling protein involved in critical functions which can cause the affected genes to be overexpressed (e.g., gene amplification) or produce mutated proteins whose activity is dysregulated (e.g., point

mutations and truncations). Examples include proteins involved in signaling pathways that are commonly activated in many physiological responses, such as growth factor receptor tyrosine kinases (RTKs; e.g., the epidermal growth factor receptor, EGFR) and lipid kinases (e.g., phosphoinositide 3-kinases, PI3Ks).[12] In 2005, erlotinib was the first reversible EGFR tyrosine kinase inhibitor (TKI) to be approved in the European Union for the treatment of patients with locally advanced or metastatic NSCLC. Gefitinib was approved in 2009 and the irreversible EGFR TKI; afatinib, was approved in 2014 for patients with NSCLC that carries activating EGFR mutations.[13] However, gefitinib and erlotinib (first-generation EGFR inhibitors) were shown the result with partial responses observed in only 10% of treated patients because it was shown to be a result of protein mutations around the EGFR pocket.[14] In 2009, Wenjun Zhou et al identified a covalent pyrimidine EGFR inhibitor by screening an irreversible kinase inhibitor library specifically against EGFR mutation (T790M) with great potential for treating NSCLC patients with one of the side chains was modified with acrylamide group.[15]

1.2 Goal and objective

We will adapt the series with novel modifications, in particular focused on the electrophilic warhead. These compounds will be compared to known EGFR drugs gefitinib, afatinib and erlotinib.[7] A range of compounds will be synthesized and assessed within biochemical and biological assays by our established academic and industrial collaborators.

1. Novel compounds based on pyrimidine scaffold will be synthesized to act as covalent inhibitors of EGFR.

2. To discovery the route of synthesis, new and potent covalent inhibitor for lung cancer that suitable for further developmental studies.

3. To better understand how suicidal protein kinase inhibitors function and how selectivity is obtained over other kinases. With this information, the design of more selective or more effective inhibitors will be possible.

1.3 Scope of the study

This research is focused on the development of methods and intellectual property on the generation of novel NSCLC treatments targeting EGFR focused on Asian individuals. The project will involve a multi-disciplinary research effort covering (a) pyrimidine-based compound synthesis and characterization, (b) computational inhibitor-target analysis and (c) experimental biological testing being performed by established collaborators in Thailand and internationally.

Chapter 2

Theory and Literature Reviews

2.1 Lung cancer

Based on the Global Cancer Incidence, Mortality and Prevalence (GLOBOCAN) 2008 estimates, about 12.7 million cancer cases and 7.6 million cancer deaths are estimated to have occurred in 2008 worldwide.[3] Asia is the most diverse and populous continent; 4.3 billion of the world's 7.1 billion people live there, and the population will increase by 1 billion by 2050. The incidence of cancer cases is estimated to increase from 6.1 million in 2008 to 10.6 million in 2030, due to ageing and growing populations, lifestyle and socioeconomic changes.[11]

Lung cancer represents a significant clinical burden worldwide. risk factors for lung cancer include exposure to several occupational and environmental carcinogens such as asbestos, arsenic, radon, and polycyclic aromatic hydrocarbons.[3] Consequently, lung cancer is the leading cause of cancer-related mortality worldwide, accounting for 19.4% of all cancer-related deaths. Non-small cell lung cancer (NSCLC) accounts for approximately 80–85% of all cases of lung cancer and is commonly diagnosed at an advanced stage of disease. NSCLC has identified driver mutations that may contribute to early carcinogenesis in more than 80% of ADC cases, including epidermal growth factor receptor (EGFR) mutations.[8]

2.2 Lung cancer drugs on market

Many advances have been made in the treatment of NSCLC over the last few decades, including improvements in cytotoxic chemotherapy regimens and the discovery

of new targeted therapies.[16] Chemotherapy is the acceptable standard treatment of advanced NSCLC; however, its outcome is still not satisfactory in terms of adverse events and patients quality of life. Furthermore, in some patients, side effects of systemic chemotherapy may interfere with their quality of life and negate the potential benefits of treatment. Recent advances in the understanding of tumor biology are starting to provide us with new tools in cancer treatment: molecularly targeted drugs.[17]

Platinum-doublet chemotherapy is considered to be the standard first-line chemotherapy for advanced or metastatic NSCLC in most centers. Addition of a third chemotherapeutic drug to the platinum-doublet significantly increased toxicity in several trials with no improvement in survival. For patients with refractory/relapsed disease, approved second-line treatments include docetaxel and pemetrexed although survival benefits with these agents are modest.[16, 18]

Gefitinib and Erlotinib (first-generation of reversible EGFR inhibitors) received accelerated approval by the US Food and Drug Administration (USFDA) for monotherapy for patients with advanced NSCLC after failure of both platinum-based chemotherapy and docetaxel.[16]

Afatinib is a second-generation of the irreversible EGFR TKI. Which is used for patients with locally advanced or metastatic NSCLC with EGFR mutations or deletion that is not respond to gefitinib and erlotinib.[13]

Osimertinib, the third generation irreversible EGFR TKI was approved in Europe in 2016 for the treatment of adult patients with metastatic EGFR T790M mutation NSCLC. The result demonstrate the superior efficiency of osimertinib over platinum chemotherapy.[13] (Figure 1)

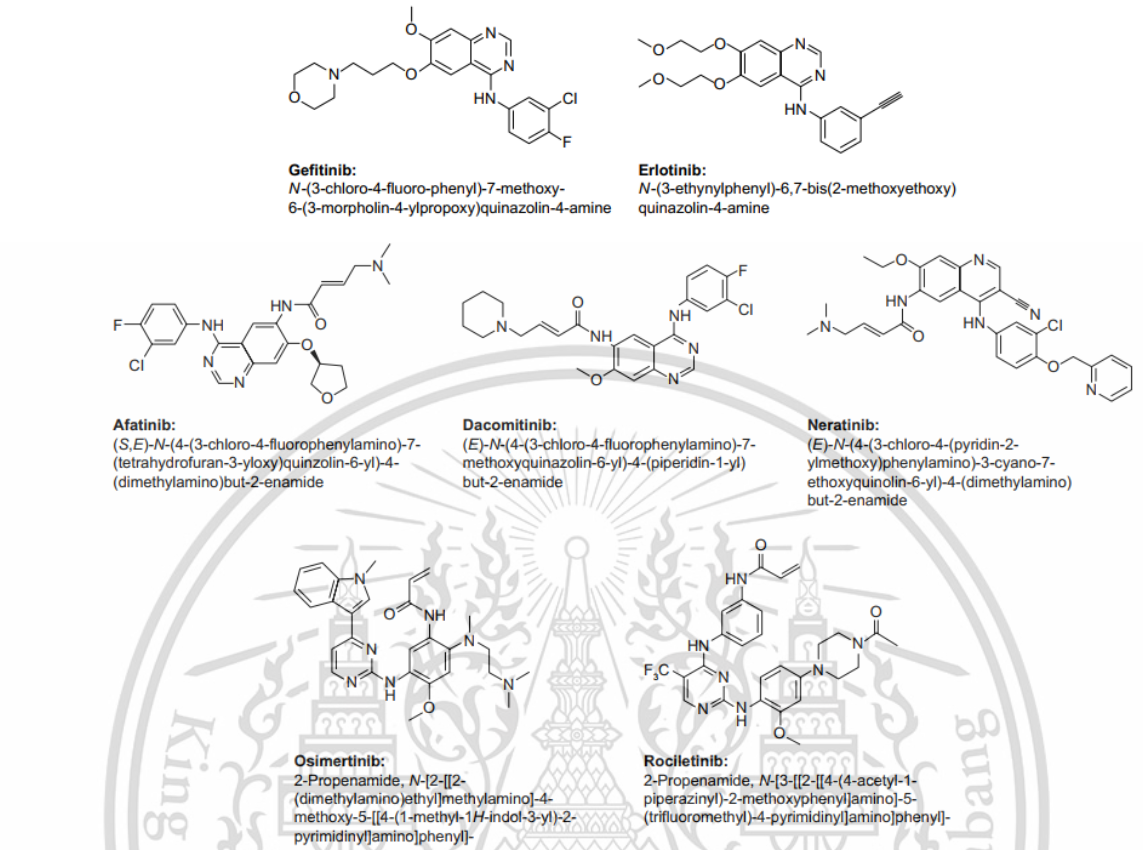

Figure 1. Structures and chemical name of known drugs cancer on the market (EGFR TKI).[7]

2.3 Targets of interesting in this study

Protein kinases are an important role in cellular signaling transduction pathways (transfer a phosphate group from ATP to a variety of amino acid residues such as tyrosine and threonine)[19] which is regulated for functional cell such as cell growth, cell transformation, differentiation, survival and cell death. A variety of diseases including cancer have dysfunctional tyrosine kinase receptors.[20]. Tyrosine kinase receptor is protein that act as receptor to growth factor ligand on a cells surface. Growth factor ligands bind to (1) extracellular domain of receptor tyrosine kinases, and the receptor is often activated by ligand-induced dimerization or oligomerization. (2) transmembrane domain is

consisting of the entirety of hydrophobic region of amino acids in the cell membrane. (3) intracellular tyrosine kinase domains, when tyrosine kinases recruit and activates with phosphorylation it induces a conformational change to an increasing of kinase activity and stimulate signal transduction for cancer cells proliferation.[21-23]

2.3.1 Epidermal growth factor receptor (EGFR)

Epidermal growth factor receptor (EGFR) is a transmembrane protein with cytoplasmic kinase activity that transduces important growth factor signaling from the extracellular milieu to the cell. Given that more than 60% of non–small cell lung carcinomas (NSCLCs) express EGFR, EGFR has become an important therapeutic target for the treatment of these tumors. Inhibitors that target the kinase domain of EGFR have been developed and are clinically active. More importantly, such tyrosine kinase inhibitors (TKIs) are especially effective in patients whose tumors harbor activating mutations in the tyrosine kinase domain of the EGFR gene.[24] EGFR (HER1, ErbB1) is a member of a family of transmembrane glycoprotein receptors that also includes HER2, HER3, and HER4 (known as ERBB2, ERBB3, and ERBB4, respectively). In normal cells, ligand binding to the extracellular domain of EGFR induces receptor homodimerization and heterodimerization, which leads to conformational changes in EGFR, activation of the intracellular tyrosine kinase domain, phosphorylation of specific tyrosine residues, and recruitment of a range of proteins, which activates downstream signaling pathways including mitogen-activated protein kinase (MAPK), phosphatidylinositol-3-OH kinase (PI3K/Akt), and the signal transducer and activator of transcription (STAT)-mediated pathways (Figure 2).[25]

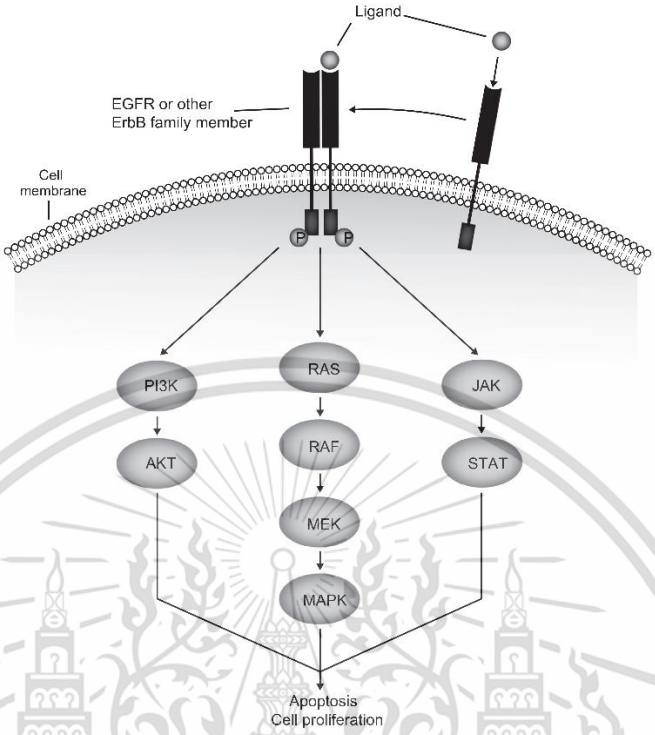

Figure 2. The EGFR Signaling transduction pathway and activation of downstream pathways regulate apoptosis and cell proliferation.[26]

2.4 Covalent kinase inhibitor

To date, the development of covalent drugs has increased significantly in many journals (Figure 3).[27] Covalent kinase inhibitors are capable of forming an irreversible, covalent bond to the kinase active site, most frequently by reacting with a nucleophilic cysteine residue.[11] Notably, covalently-bound kinase inhibitors, which target noncatalytic cysteines at the ATP binding site of protein kinases have been successfully designed as potential anticancer agents.[28] A covalent inhibitor is covalent that reacts with its target protein to form a covalent complex involved with blocking the signal process of protein. Moreover, covalent drugs have proved to be a highly profitable class of treatments for the pharmaceutical market. In fact, in 2009 three of the top selling drugs in the US (clopidogrel, lansoprazole and esomeprazole) are covalent inhibitors. However, a common element in the discovery of covalent drugs is that they were identified not by design but by

serendipity, with their covalent mechanism of action becoming apparent only after their clinical utility had been well established. The earliest example is aspirin, which was first marketed over 100 years ago (Figure 4).[29]

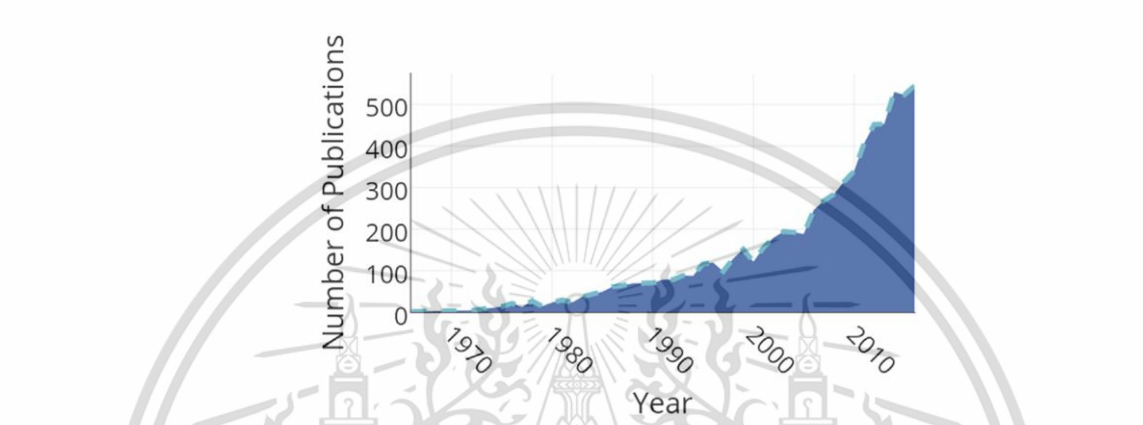

Figure 3. Number of publications obtained from the search of 'covalent drugs' in SciFinder.[27]

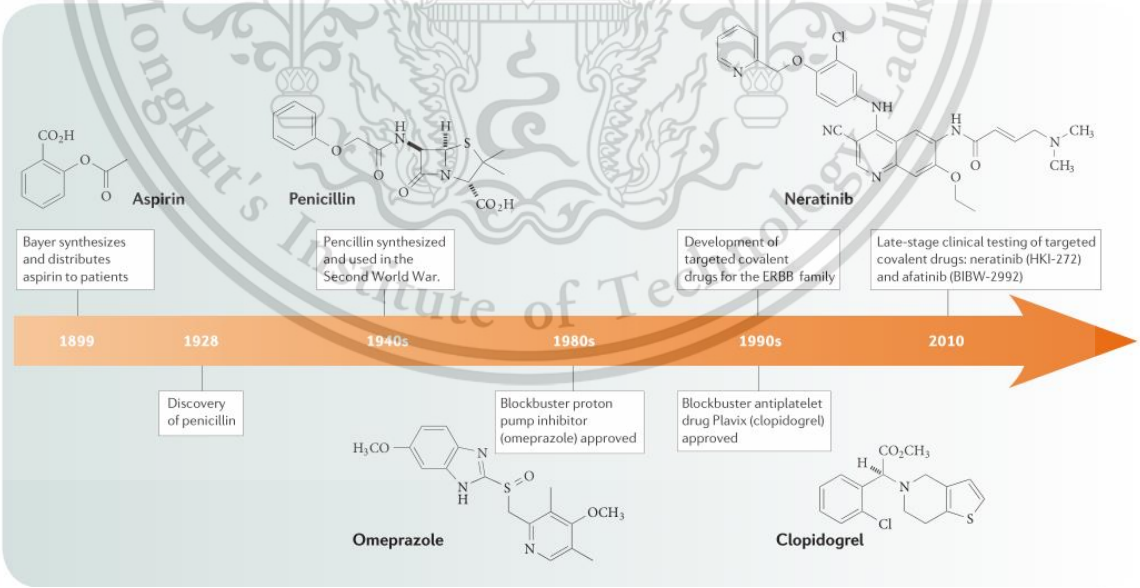

Figure 4. Historical examples of covalent drugs on the pharmaceutical market.[29]

A small molecule of covalent inhibitor is designed not only to bind to a protein with traditional reversible (noncovalent) interactions, but also to undergo a forming bond that produces a durable of action between drug and protein linkage. Thus, covalent inhibition is the extended duration of action that can result from the neutralization of a target under nonequilibrium kinetics (Figure 5).[30, 31] Formation of a covalent bond can mean that the effect of covalent inhibitors can remain long after all the free drug has been cleared from the body. As shown in Figure 5, we can see the different types of inhibitor on pharmacodynamic (PD) simulation. the percentage of a noncovalent inhibitor is rapidly decays. On the contrary, covalent reversible inhibitor is slowly decays with a much longer period compare with noncovalent inhibitor. In recent years, the pursuit of irreversible, covalent inhibitors as drug candidates has gained renewed impetus in the pharmaceutical industry. Potential advantages of covalent inhibitors over conventional reversible inhibitors include the possibility of achieving increased biochemical potency and isoform selectivity through targeted covalent modification of a specific amino acid residue in the active site of the receptor or enzyme. Along with the irreversible inhibitor follows the same trend even in short period of exposure can induce permanent inhibition of the target with no need for additional doses.[27],[32]

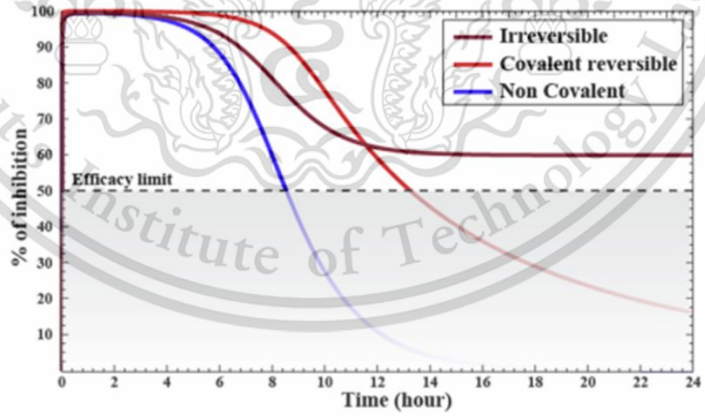

Figure 5. Pharmacodynamic (PD) simulation of an effect pharmacokinetics (PK) of a given target by different types of inhibitors (bottom).[27]

2.5 Structure based-design

Structure based-design is the process whereby compounds to a target a particular protein are designed using 3D structural information of the target.[33] This can range from knowledge gained from simple 3D X-ray structures of the ligand, NMR based protein-ligand complexes to theoretical molecular simulations of a protein-ligands complex over a certain timescale. The key feature of this method is to utilize structural information to guide the design and synthesis of a later generation of ligands.

In this research the huge amount of information is available on EGFR which will be used to help guide the design of new 2,4-Dichloropyrimidine compounds. The compounds have undergone using 3D structural overlays from related X-ray structures-templates taken from the Protein data bank. This includes the recently reported created a crystal structure of common kinase inhibitor pyrimidine-core scaffolds where one of the side chains was modified with an acrylamide group in the active site of EGFR kinase which were used in the EGFR docking (Figure 6). This allows us to confirm how the molecules fit within the active sites of these proteins and the specific pharmacophoric requirements/constraints. This has facilitated the selection of a range of different chemical building blocks, which have been subsequently purchased, to explore the SAR within the pocket.

Wenjun Zhou et al., 2009 had hypothesized that the anilinoquinazoline scaffold may not be the most potent or specific for inhibiting EGFR T790M because it relies on the small size and hydrogen bonding interactions with the gatekeeper threonine of wild-type (WT EGFR). They prepared a focused library of common kinase inhibitor pyrimidine core scaffolds where one of the side chains was modified with an acrylamide group. The anilinopyrimidine core of crystal structure forms a bidentate hydrogen bonding interaction with the ‘hinge’ residue Met 793. The aniline ring forms a hydrophobic interaction with the a-carbon of Gly 796. The EGFR kinase is shown in a ribbon representation (blue) with the bound inhibitor in yellow. Side-chain and main-chain atoms are shown for selected residues that contact the compound. Expected hydrogen bonds to the backbone amide and

carbonyl atoms of Met 793 are indicated by dashed lines. Note also the covalent bond with Cys 797 (Figure 6).

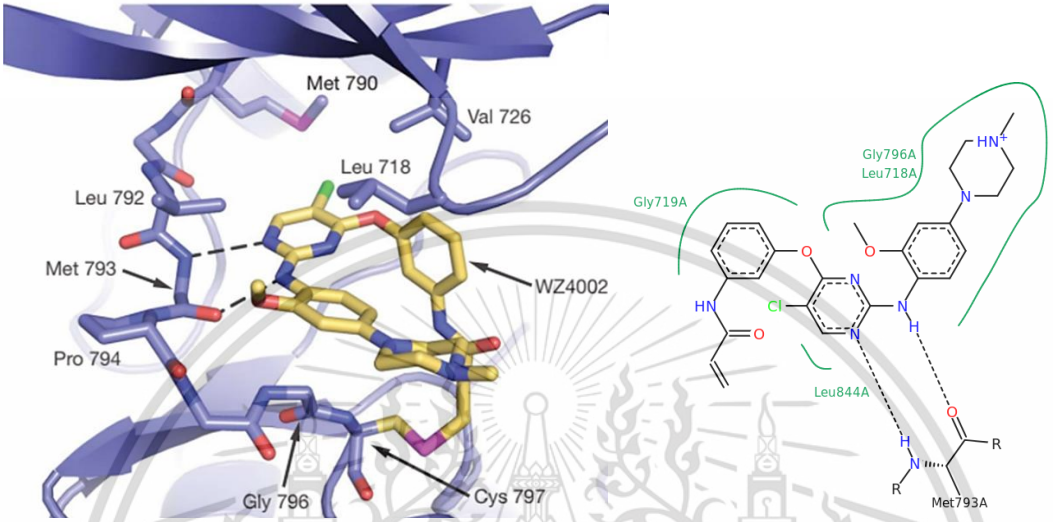

Figure 6. Crystal Structure of EGFR kinase compound (WZ4002) in development indicating the key interactions between ligand and protein. (PDB data: 3IKA) [15]

2.6 Synthesis of protein kinase inhibitors

The goal of medicinal drug design is to develop novel templates as rapidly as possible and ensure that any route of synthesis is adaptable such that a diverse range of molecules can be made from a range of common building blocks and catalysts. This has led to the industry utilizing a much more limited selection of organic chemistry transformations suitable for combinatorial chemistry and have been well documented. A typical medicinal chemistry project will focus on the characterization of the chemical space surrounding a hit series using well established, reliable synthetic methods. Only after demonstrating the potential of the series is an investment made into more sophisticated, less reliable synthetic procedure. A typical medicinal chemistry project will focus on the characterization of the chemical space surrounding a hit series using well established, reliable synthetic methods. Only after demonstrating the potential of the series is an investment made into more sophisticated, less reliable synthetic procedures. The project

proposed herein will therefore use general heterocyclic chemistry methods,[34, 35] common halide, amine and boronic building blocks to develop an SAR strategy.

Chapter 3

Materials and Methods

3.1 Materials

3.1.1 Instruments

^{1}H NMR spectra and ^{13}C NMR were recorded on a Varian instrument at 400 MHz and 100 MHz respectively. Chemical shifts (δ) were reported in parts per million (ppm) using TMS as the the residual solvent line as the internal standard. ^{1}H NMR spectra were measured in $CDCl_3$ and DMSO, the solvent residual peaks are 7.26 ppm and 2.50 ppm respectively.

The coupling constant (*J*) are given in Hz, and the patterns are designed as singlet (s), doublet (d), doublet of doublet (dd), triplet (t), quartet (q), multiplet (m) and broad (br)

Mass spectra (MS) were performed on Agilent 1100 HPLC instrument coupled to a LC|MSD Trap mass spectrometer, in ESI(+) mode or APCI mode or using High Resolution Mass Spectrometer (HRMS) were measured on Bruker micrOTOF-Q III in ESI(+) mode. All compounds shall demonstrate a purity >95% based on a UV absorbance HPLC chromatogram (Agilent 1100 system, Sunshell C8).

IR spectra were recorded on Fourier Transform Infrared Spectrometer (FTIR) PerkinElmer Spectrum Two. All compounds was testing in the zone 4000-400 cm^{-1} and are reported between % transmittance and cm-

3.1.2 Column & Thin Layer Chromatography

All reactions were monitored by thin layer chromatography (TLC) TLC Silicycle UltraPure Silica gels with UV light visualization (254 nm). Purification of the compounds by column chromatography was performed using silica gel 60 (40-63 μm).

3.1.3 Chemical reagents

Reagents and solvents obtained from commercial suppliers were used without further purification.

3.1.4 Cell lines and reagents

The human epidermal carcinoma cell line A431 were obtained from the American Type Culture Collection (ATCC, Manassas, VA, USA). Cells were grown in DMEM media (Gibco) supplemented with 10% FBS (HyClone) and maintained as monolayer culture in a humidified incubator with 5% CO_2 at 37 °C.

3.2 Methods

3.2.1 Structure based-design

The compounds have undergone using Discovery Studio v.4.1.0.14169 using 3D structural overlays from related X-ray structures-templates taken from the Protein data bank (PDB). Alignments are assessed by comparing to a structure-based alignment, derived from structural overlays of the target and template. This includes the recently reported created a crystal structure of common kinase inhibitor pyrimidine-core scaffolds where one of the side chains was modified with an acrylamide group in the active site of EGFR kinase which were used in the EGFR docking. This allows us to confirm how the molecules fit within the active sites of these proteins.

3.2.2 General procedure for the preparation of intermediate compounds (1-3) and final compound (4)

Intermediates and final compound were synthesized using methodology as described in Scheme 1.

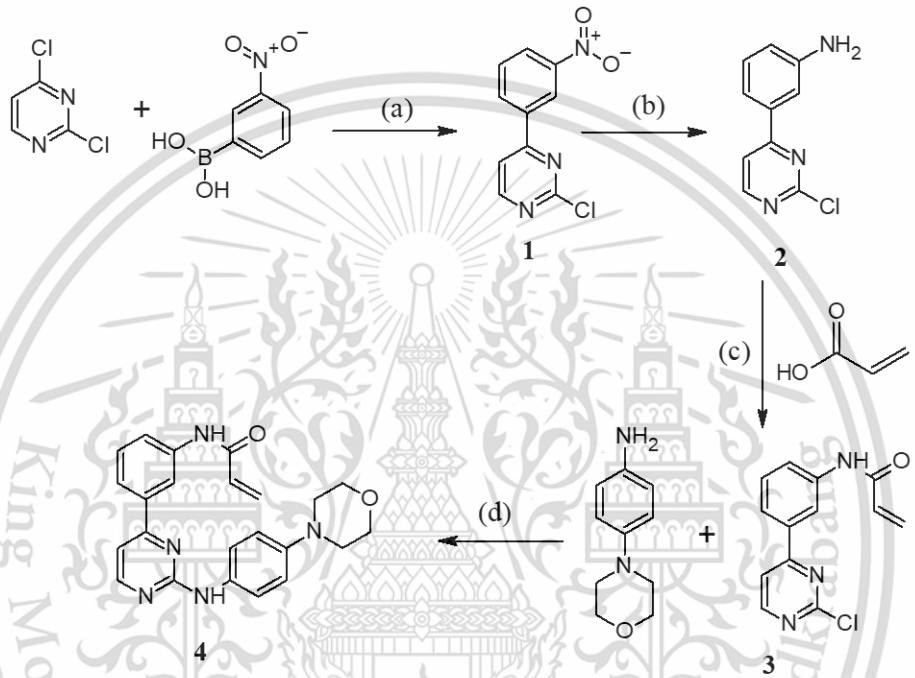

Scheme 1. The route of synthesis of compound **4**. (a) $Pd(PPh_3)_4$, Na_2CO_3, N_2 gas, 1,4-dioxane, 80°C, overnight, (b) $SnCl_2$, ethanol, 40°C, overnight, (c) acrylic acid, HATU, DIPEA, acetonitrile, 0°C to room temperature, 2 hours, (d) 4-morpholinoaniline, TFA, propan-2-ol, 100°C, overnight.

3.2.2.1 Synthesis of 2-chloro-4-(3-nitrophenyl) pyrimidine (1)

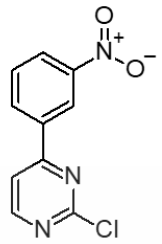

A mixture of 2,4-dichloropyrimidine (1.5 equiv.), 3-nitrophenylboronic acid (1 equiv.) and Na_2CO_3 (10 mL of 2M aq. solution) was dissolved with 1,4-dioxane was purged with argon gas for 5 min. and then tetrakis(triphenylphosphine)palladium (0) (0.01 equiv.) was added to a reaction mixture under the nitrogen atmosphere. The mixture was stirred at 80°C for overnight. The cooled mixture was diluted with water and the solution was collected by extracted with ethyl acetate, dried over anhydrous sodium sulfate and concentrated under reduced pressure.

3.2.2.2 Synthesis of 3-(2-chloropyrimidin-4-yl)aniline (2)

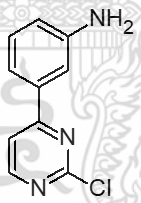

2-chloro-4-(3-nitrophenyl) pyrimidine (1.0 equiv.) and tin(II) chloride (5.0 equiv.) were heated overnight in ethanol at 40°C. The mixture was cooled and diluted with saturated Na_2CO_3 and DCM. The reaction mixture was filtered through filter paper. The aqueous layer was extracted with DCM. The combined organic extracts were dried and concentrated under reduced pressure.

3.2.2.3 Synthesis of *N*-[3-(2-chloropyrimidin-4-yl)phenyl] prop-2-enamide (3)

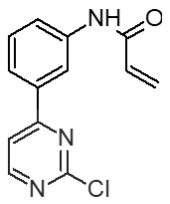

A solution of 3-(2-chloro pyrimidin-4-yl)aniline (1.0 equiv.), acrylic acid (1.2 equiv.), 1-[Bis(dimethylamino)methylene]-1H-1,2,3-triazolo[4,5-b]pyridinium3-oxidhexafluorophosphate (HATU) (1.5 equiv.) and in acetonitrile was stirred at 0°C. Then *N,N*-diisopropylethylamine (1.2 equiv.) was added into a solution. The mixture was allowed to warm at room temperature for 2 hours then diluted with DCM and washed with saturated aqueous $NaHCO_3$. The organic layer was dried over anhydrous sodium sulfate and concentrated under reduced pressure. The product was purified by column chromatography.

3.2.2.4 Synthesis of the final compound (4)

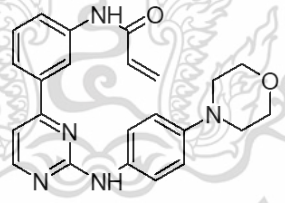

A mixture of *N*-[3-(2-chloropyrimidin-4-yl)phenyl] prop-2-enamide (1.0 equiv.), 4-morpholinoaniline (1.0 equiv.)and trifluoroacetic acid (1.2 equiv.) were dissolved in propan-2-ol and heated at 100°C in a sealed tube for overnight. The reaction mixture was concentrated in vacuo, re-dissolved in ethyl acetate and washed with saturated $NaHCO_3$ and extract. The organic layer was collected, dried over anhydrous sodium sulfate and concentrated under reduced pressure. The residue was purified by column chromatography.

3.2.3 General procedure for the preparation of intermediate compounds (5-8) and final compound (9)

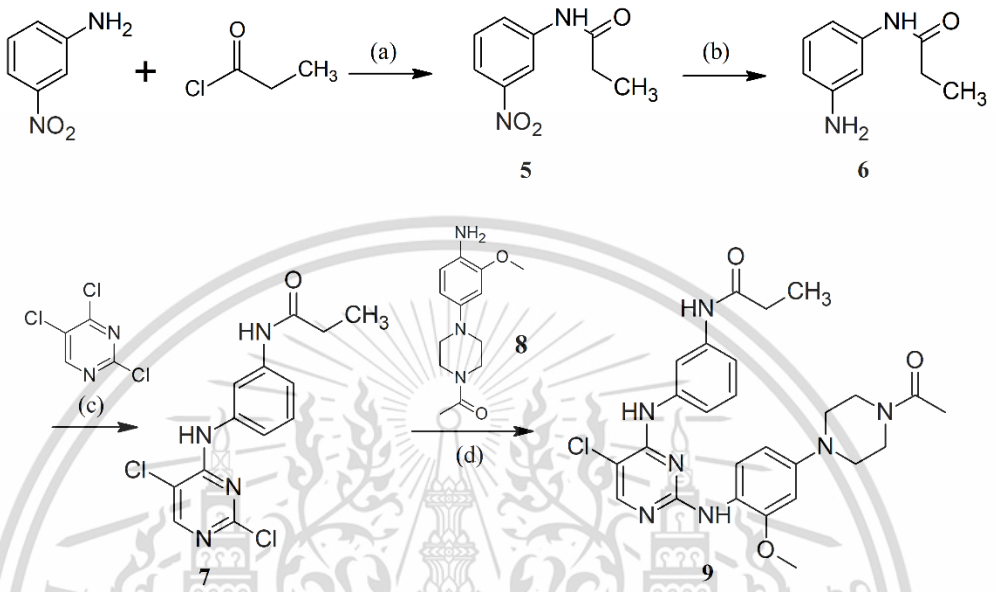

Scheme 2. The route of synthesis of compound **9**. (a) DIPEA, DCM, 0°C, N_2 gas, 3 hours, (b) $SnCl_2$, ethanol, 40°C, overnight, (c) TEA, THF, room temperature, 4 hours, (d) 1-[4-(4-amino-3-methoxyphenyl)piperazin-1-yl]ethenone (compound **8**), TFA, propan-2-ol, 100°C, overnight.

3.2.3.1 Synthesis of N-(3-nitrophenyl) propenamide (5)

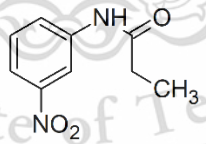

Propanoyl chloride (1.5 equiv.) was added dropwise to 3-Nitroaniline (1 equiv.) and DIPEA (1.1 equiv.) in DCM (15 mL) at 0°C under nitrogen. The resulting suspension was stirred at 0 °C for 1 h and then allowed to warm to room temperature. The reaction mixture was diluted with water (15 mL) and reduced in vacuo. The resultant crude product was dissolved in DCM (20 mL) and MeOH (5 mL) and washed with water and saturated brine. The organic layer was dried and evaporated. The crude product was purified by

column chromatography. Pure fractions were evaporated to dryness to obtained N-(3-nitrophenyl) propenamide.

3.2.3.2 Synthesis of N-(3-aminophenyl)propanamide (6)

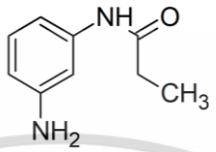

N-(3-nitrophenyl) propenamide (1.0 equiv.) and tin(II) chloride (5.0 equiv.) were heated overnight in ethanol at 40°C. The mixture was cooled and diluted with saturated Na_2CO_3 and DCM. The reaction mixture was filtered through filter paper. The aqueous layer was extracted with DCM. The combined organic extracts were dried and concentrated under reduced pressure.

3.2.3.3 Synthesis of N-[3-[(2,5-dichloropyrimidin-4-yl)amino]phenyl]propanamide (7)

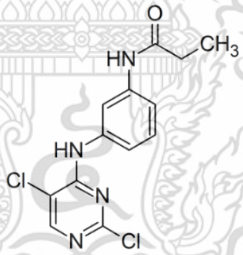

A solution of 2,4,5-trichloropyrimidine (1.0 equiv.) in tetrahydrofuran (THF), N-(3-aminophenyl)propenamide (1.0 equiv.) and triethylamine (Et_3N) were added. The reaction proceeded at room temperature for 4 hours. The mixture was concentrated in vacuo, re-dissolved in ethyl acetate and washed with saturated $NaHCO_3$ and extract. The organic layer was collected, dried by anhydrous Na_2SO_4, filtered, and dried under reduced pressure to give the compound as a solid.

3.2.3.4 Synthesis of 1-(4-(3-methoxy-4- nitrophenyl)piperazin-1-yl)ethanone (8)

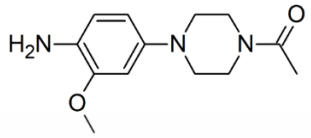

1-Acetylpiperazine (1.1 equiv.) and DIPEA (1.2 equiv.) were added to a stirred solution of 4-fluoro-2-methoxy-1-nitrobenzene (1.0 equiv.) dissolved in DMA under argon. The resulting solution was stirred at 90°C overnight. The reaction mixture was allowed to cool to room temperature and quenched with water. The aqueous layer was extracted with EtOAc (×3). The combined organic layers were washed with water (×2) and brine, dried by anhydrous Na_2SO_4, and concentrated to afford 1-(4-(3-methoxy-4-nitrophenyl)piperazin-1-yl)ethenone.[36]

A suspension of 1-(4-(3-methoxy-4-nitrophenyl)piperazin-1-yl)ethenone (1.0 equiv.) and 10% palladium on carbon (Pd/C) in ethanol was stirred under hydrogen at room temperature for 6 hours. The resulting suspension was filtered through Celite® 545, and the filtrate was concentrated to dryness to afford 1-(4-(4-amino-3-methoxyphenyl)piperazin-1-yl)ethenone.

3.2.3.5 Synthesis of final compound (9)

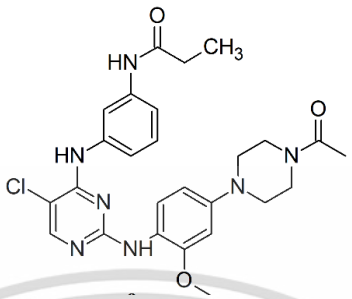

A mixture of N-[3-[(2,5-dichloropyrimidin-4-yl)amino]phenyl]propanamide (1.0 equiv.), 1-(4-(4-amino-3-methoxyphenyl)piperazin-1-yl)ethenone (1.2 equiv.) and trifluoroacetic acid (1.2 equiv.) were dissolved in propan-2-ol and heated at 100°C in a sealed tube for overnight. The reaction mixture was concentrated in vacuo, redissolved in ethyl acetate and washed with saturated $NaHCO_3$ and extract. The organic layer was collected, dried over anhydrous sodium sulfate and concentrated under reduced pressure. The residue was purified by column chromatography to obtained compound **9**.

3.2.4 The route of synthesis of acid chloride

From 3.2.2.3, the %yield of the reaction with HATU is rather low. Therefore, we decided to explore the possibility of using a route of synthesis whereby the carboxylic acid group was converted into the corresponding acid chloride. This was necessary due to the fact that the desired acid chloride cannot be imported into Thailand. The most frequently used method for the preparation of acid chlorides is the use of thionyl chloride and oxalyl chloride as chlorinating agents. Oxalyl chloride is the second organic chlorinating reagent suitable to convert α,β-unsaturated carboxylic acids to the corresponding acid chlorides. [37]

In the follow up investigation we employed the procedure from L. Ding et al.[38]. Under a nitrogen, $(COCl)_2$ (5.0 equiv.) was added by syringe to acrylic acid (1.0 equiv.) at room temperature with rapid stirring, which resulted in the vigorous evolution of CO_2 (g), CO (g), and HCl (g). After 6 hours, the evolution of gases had ceased. The excess $(COCl)_2$ was removed in vacuo to yield acryloyl chloride. The result found the %yield of product

still low and the data result from ^{1}HNMR shown that the conversion of acrylic acid did not fully convert to acid chloride.

Then we design the experiment to explore the route of synthesis with the addition from *L. Wimmer et al.*[39], by adding few drops of dimethylformamide (DMF) with various time of the reaction to evaluate the effect of DMF and the reaction time on the synthesis to compare the result. For the transformation of acrylic acid into acryloyl chloride, The reaction mixture of acrylic acid and DMF as a catalyst were mixed under the N_2 atmosphere at 25° with rapidly stirred. The oxalyl chloride ($(COCl)_2$) was added dropwise by syringe to the mixture. Stirring continued for the various time and the excess oxalyl chloride are removed in vacuo.

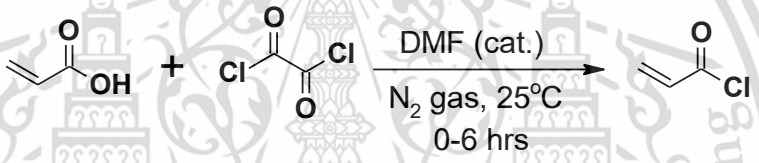

Scheme 3. The reaction conditions on the conversion of acrylic acid

3.2.5 Biological testing procedure

The inhibition was determined by using Antibody Beacon™ Tyrosine Kinase Assay Kit (A-35725; Invitrogen, USA): for the EGFR kinase assay were constituted and performed in a similar manner except for the following differences in reagents.[40] The detection complex contained the following components in 1X kinase assay buffer (50 mM Tris-HCl pH 7.5, 10 mM $MgCl_2$, 1 mM EGTA, 0.01% Brig and 2 mM DTT), 0.0267 mg/ml poly (Glu:Tyr), 6.7 nM anti-phosphotyrosine antibody, 0.33 nM Oregon Green 488 ligand and 0.5 mM ATP. To the reaction was added with 12.5 µl of test compounds and 12.5 µl of EGFR enzyme (10 ng enzyme/reaction). After that, 25 µl of the detection complex was added into each well. The mixture solution was analyzed for 1.5 hours at 30°C in a fluorescence microplate reader using excitation at 485 nm and emission at 535 nm using an Infinite F200 fluorescence microplate reader (Tecan). The IC_{50} data was obtained by

fitting using Prism 6.0 (GraphPad Software Inc., San Diego, CA, USA). Erlotinib and Afatinib were used as positive controls.

3.2.6 Cytotoxicity assay

The cell viabilities of cancer cell lines (A431) exposed to the screened overexpress-EGFR were evaluated by the MTT assay. The cell suspension (100 µL) was seeded into 96-well plates at a density of 5,000 cells/well and then incubated for 24 hours under normal culture conditions before the addition of the respective test compound at various concentrations and incubated for another 72 hours. Then, 10 µL of fresh MTT solution (5mg/mL) was added to each well and incubated at 37°C in a humidified incubator with 5% CO_2 for 2 hours, before the reaction was stopped by adding 100 µL of DMSO. The absorbance was measured at 570 nm with correction for background at 690 nm using a microplate spectrophotometer system (Infinite M200 micro-plate reader, Tecan, Männedorf, Switzerland).[41]

3.2.7 Solubility

An equilibrium shake-flask technique was used to determine the solubility of sample in phosphate buffer solution (PBS) at pH 7.4. Approximately 1 mg of sample was placed in a 10 mL glass screw top vial and dissolved in 1 mL of 0.02 M PBS at pH 7.4. The solution was sonicated for 1 hr. followed by shaking for 6 hrs. (IKA HS 260). The saturated solution was filtered using a nylon syringe filter. A standard solution of each sample was prepared by dissolving a weighed amount of sample in 1 mL of DMSO. The concentration of sample dissolved in the PBS solution was determined by comparing the area under the curves for the PBS and DMSO standard using an AGILIENT 1100 series HPLC with a SUNSHELL C8 column (Chromanik Technologies Inc. Japan). A 100 µL injection of the aqueous sample and 5 µL of DMSO solution (pre-diluted 100-fold using DMSO) were used.

Chapter 4

Results and Discussion

4.1 Design

The binding mode of compound **4** was obtained by modelling it into the crystal structure of a complex containing a diamino pyrimidine covalent inhibitor with EGFR (PDB: 3IKA) (Figure 7). The scaffold-based superposition was undertaken with minimization in Discovery Studio. The compound is predicted to bind to EGFR via H-bond interaction with the hinge region and a covalent bond with Cys797. This model will allow us to explore the incorporation of new modification, including Michael acceptor groups to improve the series potency of EGFR.

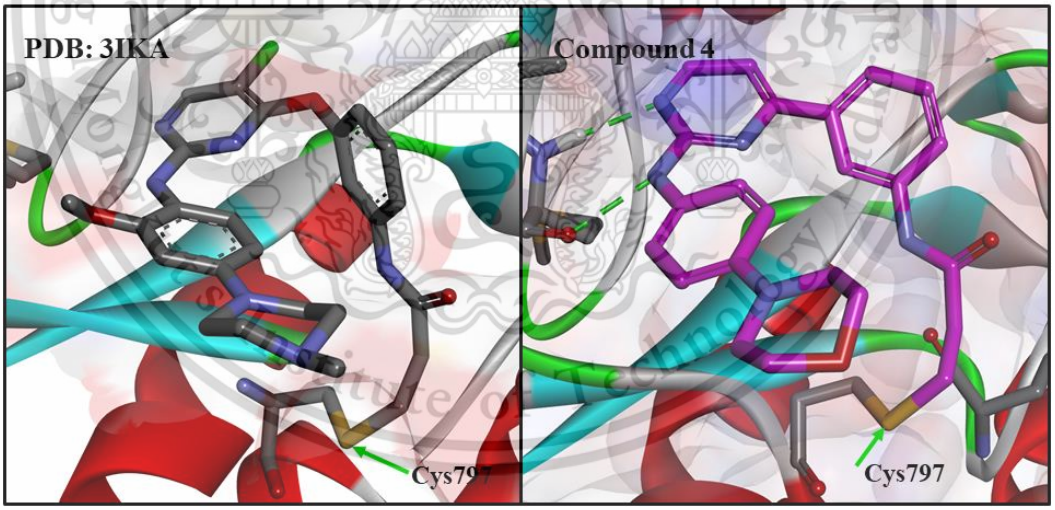

Figure 7. Comparison of binding mode of EGFR crystal structure (PDB: 3IKA) and the compound **4** in EGFR pocket site. This docking has been used to guide the next stage of compound design.

4.2 Synthesis chemistry

4.2.1 Synthesis of 2-chloro-4-(3-nitrophenyl) pyrimidine (1)

The crude product was purified by chromatography (56% yield) as a yellow solid. ^{1}H NMR (400 MHz, DMSO-d_6) δ 8.95 (d, J = 2.2 Hz, 1H), 8.94 (s, 1H), 8.64 (dd, J = 7.9, 0.9 Hz, 1H), 8.48-8.43 (m, 1H), 8.35 (d, J = 5.3, 1H), 7.90 (t, J = 8.0 Hz, 1H). ^{13}C NMR (100 MHz, DMSO-d_6) δ 164.4, 162.4, 161.0, 149.0, 136.7, 134.1, 131.4, 126.9, 122.3, 117.3. MS-ESI: m/z $[M+H]^+$ 236.6 found 236.0.

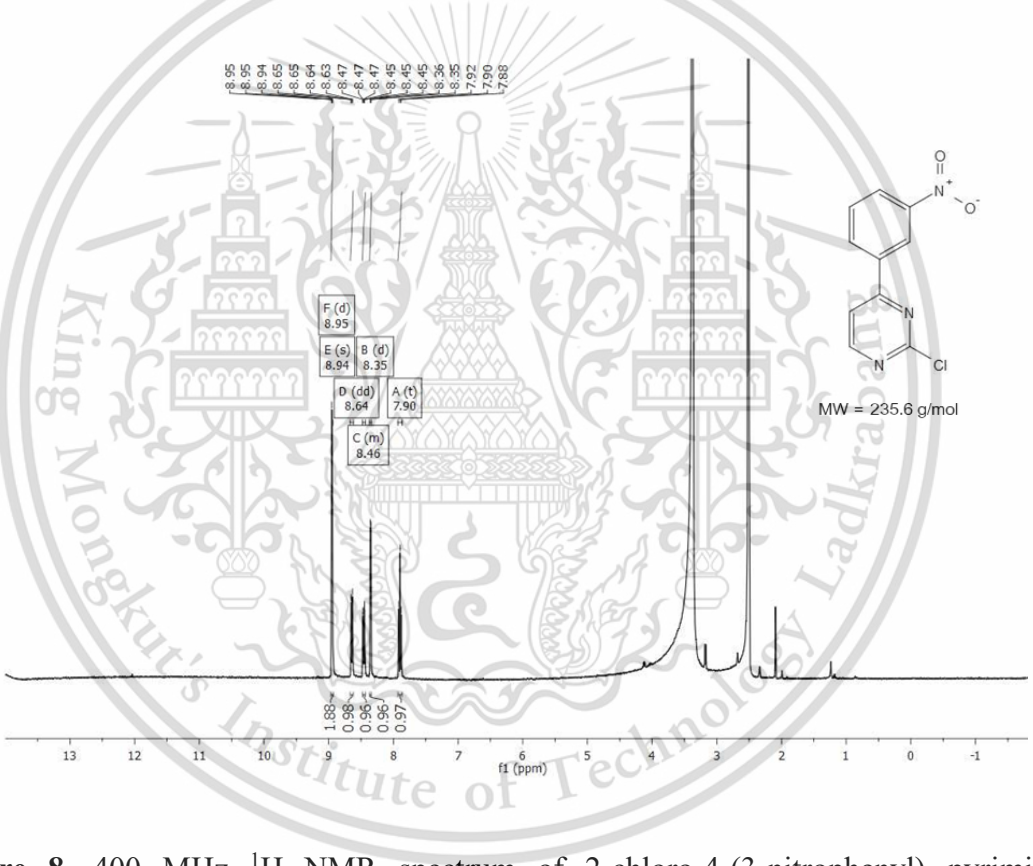

Figure 8. 400 MHz ^{1}H NMR spectrum of 2-chloro-4-(3-nitrophenyl) pyrimidine (compound **1**)

4.2.2 Synthesis of 3-(2-chloropyrimidin-4-yl)aniline (2)

The solid compound was collected to afford the product (69% yield). ^{1}H NMR (400 MHz, DMSO-d_6) δ 8.76 (d, J = 5.3 Hz, 1H), 7.98 (d, J = 5.3 Hz, 1H), 7.42 (t, J = 2.0 Hz, 1H), 7.29 (ddd, J = 7.7, 1.6, 1.0 Hz, 1H), 7.20 (t, J = 7.8 Hz, 1H), 6.78 (ddd, J = 7.9, 2.3, 0.9 Hz, 1H), 5.41 (s, 2H). ^{13}C NMR (100 MHz, DMSO-d_6) δ 167.4, 161.4, 160.9, 150.0, 135.5, 130.2, 118.0, 116.3, 115.3, 112.4. MS-ESI: m/z $[M+H]^+$ 206.6 found 206.1.

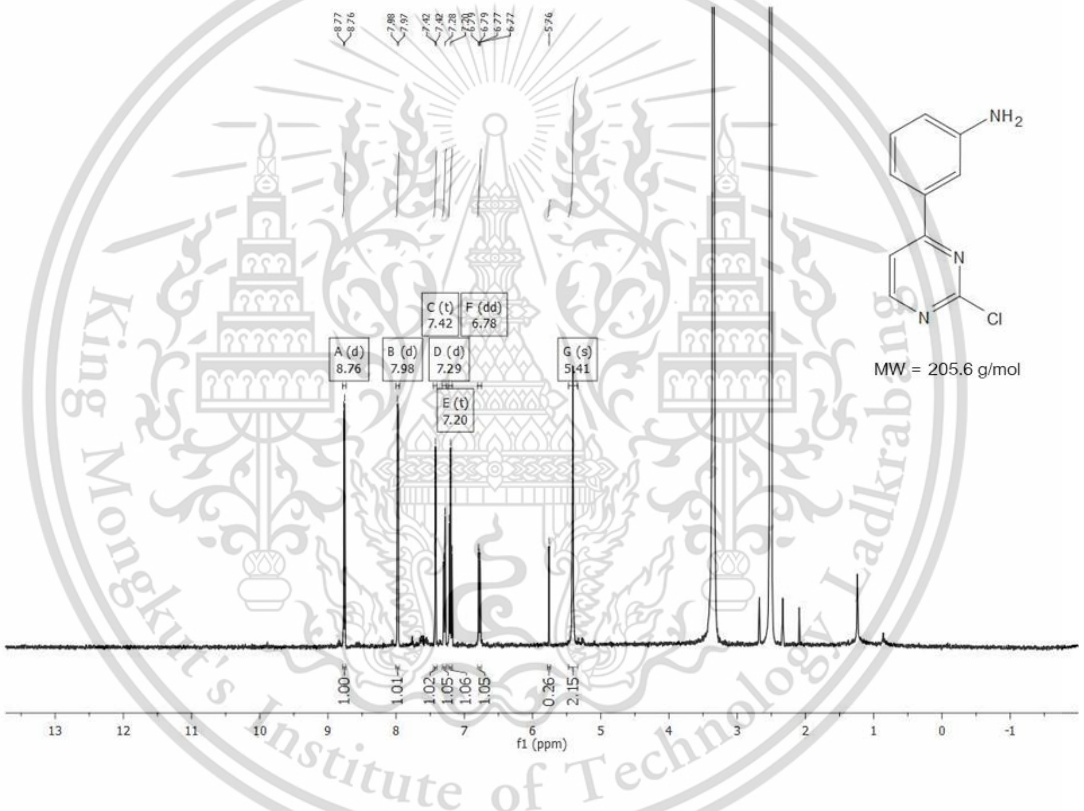

Figure 9. 400 MHz ^{1}H NMR spectrum of 3-(2-chloropyrimidin-4-yl)aniline (compound **2**)

4.2.3 Synthesis of *N*-[3-(2-chloropyrimidin-4-yl)phenyl] prop-2-enamide (3)

A light-yellow solid was collected to afford the product (26% yield). ^{1}H NMR (400 MHz, DMSO-d_6) δ 10.44 (s, 1H), 8.84 (d, J = 5.3 Hz, 1H), 8.48 (t, J = 1.8 Hz, 1H), 8.10 (d, J = 5.3 Hz, 1H), 8.00 (dd, J = 8.1, 1.4 Hz, 1H), 7.89 (dd, J = 7.9, 0.6 Hz, 1H), 7.54 (t, J = 8.0 Hz, 1H), 6.47 (dd, J = 17.0, 10.1 Hz, 1H), 6.31 (dd, J = 17.0, 2.0 Hz, 1H), 5.81 (dd, J = 10.0, 2.0 Hz, 1H). ^{13}C NMR (100 MHz, DMSO-d_6) δ 166.4, 163.9, 161.8, 161.0, 140.4, 135.6, 132.1, 130.3, 127.9, 123.2, 123.0, 118.2, 116.6. MS-ESI: m/z $[M+H]^+$ 260.7; found, 260.1.

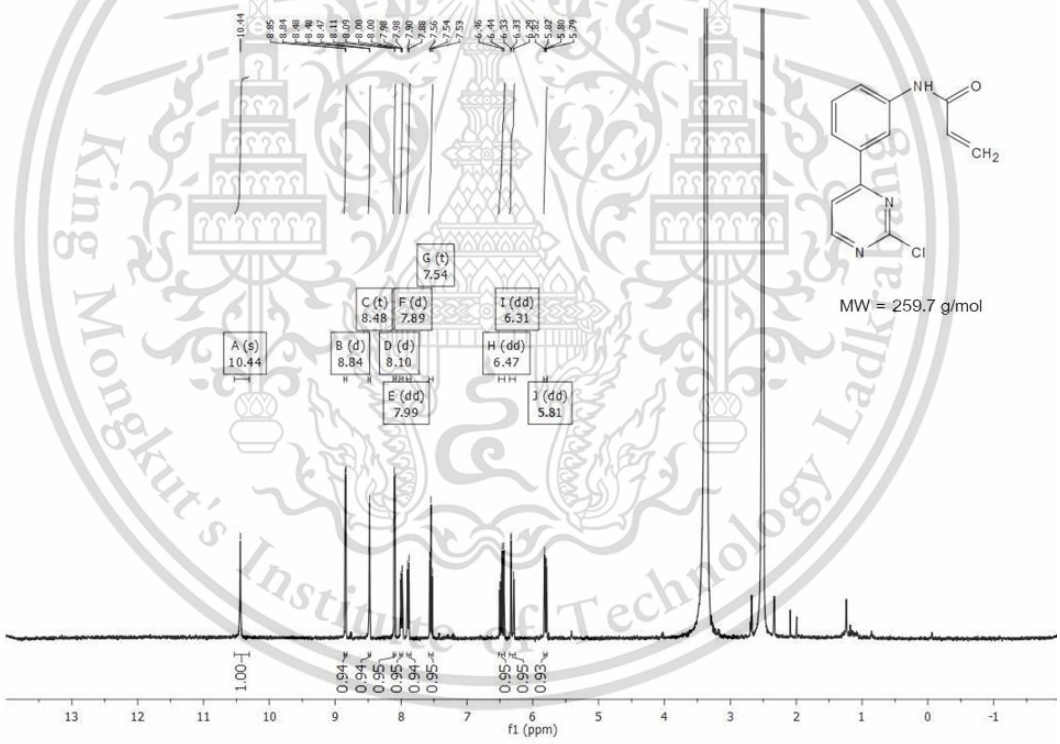

Figure 10. 400 MHz ^{1}H NMR spectrum of *N*-[3-(2-chloropyrimidin-4-yl)phenyl] prop-2-enamide

4.2.4 Synthesis of the N-[3-(2-[4-(morpholin-4-yl)phenyl]aminopyrimidin-4-yl)phenyl]prop-2-enamide (compound 4)

A brown solid was collected to afford the product **4** (19% yield). ^{1}H NMR (400 MHz, DMSO-d_6) δ 10.35 (s, 1H), 9.43 (s, 1H), 8.54 (s, 1H), 8.50 (d, J = 5.2 Hz, 1H), 7.82 (d, J = 7.8 Hz, 1H), 7.77 (d, J = 7.5 Hz, 1H), 7.71 (d, J = 9.0 Hz, 2H), 7.50 (t, J = 7.9 Hz 1H), 7.24 (d, J = 5.2 Hz, 1H), 6.95 (d, J = 9.1 Hz, 2H), 6.49 (dd, J = 17.0, 10.1 Hz, 1H), 6.31 (dd, J = 17.0, 2.0 Hz, 1H), 5.81 (dd, J = 10.1, 1.9 Hz, 1H), 3.77-3.73 (m, 4H), 3.09-3.00 (m, 4H). ^{13}C NMR (101 MHz, DMSO-d_6) δ 163.8, 160.8, 159.5, 146.6, 140.0, 138.0, 133.5, 132.3, 129.8, 127.6, 122.6, 122.1, 120.7, 118.3, 116.2, 107.7, 66.7, 49.8. HRMS-ESI: m/z calcd for $C_{23}H_{24}N_5O_2$ $[M+H]^+$ 402.1925; found, 402.1953. HPLC purity = 96%, R_t 2.793 min.

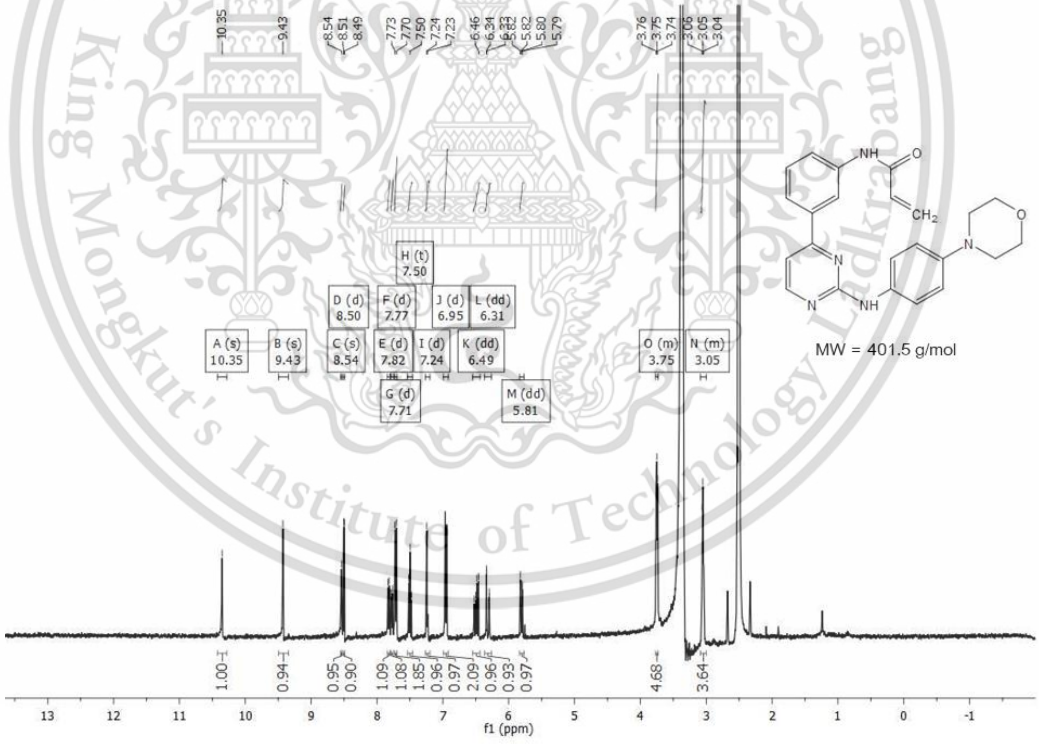

Figure 11. 400 MHz ^{1}H NMR spectrum of N-[3-(2-[4-(morpholin-4-yl)phenyl]aminopyrimidin-4-yl)phenyl]prop-2-enamide (compound **4**).

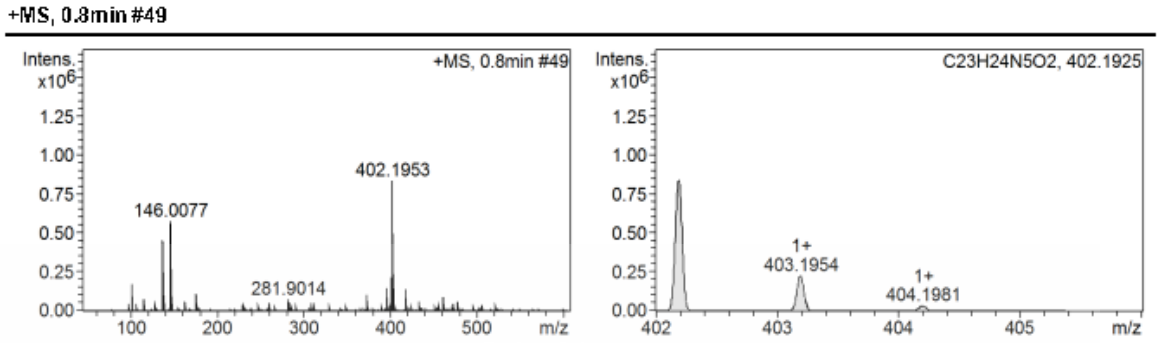

Figure 12. HRMS-ESI Mass spectrum of N-[3-(2-[4-(morpholin-4-yl)phenyl]aminopyrimidin-4-yl)phenyl]prop-2-enamide (compound **4)**

4.2.5 Synthesis of N-(3-nitrophenyl) propenamide (5)

A yellow solid was collected to afford the compound **5** (65% yield). ^{1}H NMR (400 MHz, DMSO-d_6) δ 10.35 (s, 1H), 8.64 (t, J = 2.0 Hz, 1H), 7.94 – 7.84 (m, J = 9.5, 7.8, 1.7 Hz, 2H), 7.59 (t, J = 8.2 Hz, 1H), 2.38 (q, J = 7.5 Hz, 2H), 1.11 (t, J = 7.5 Hz, 3H).

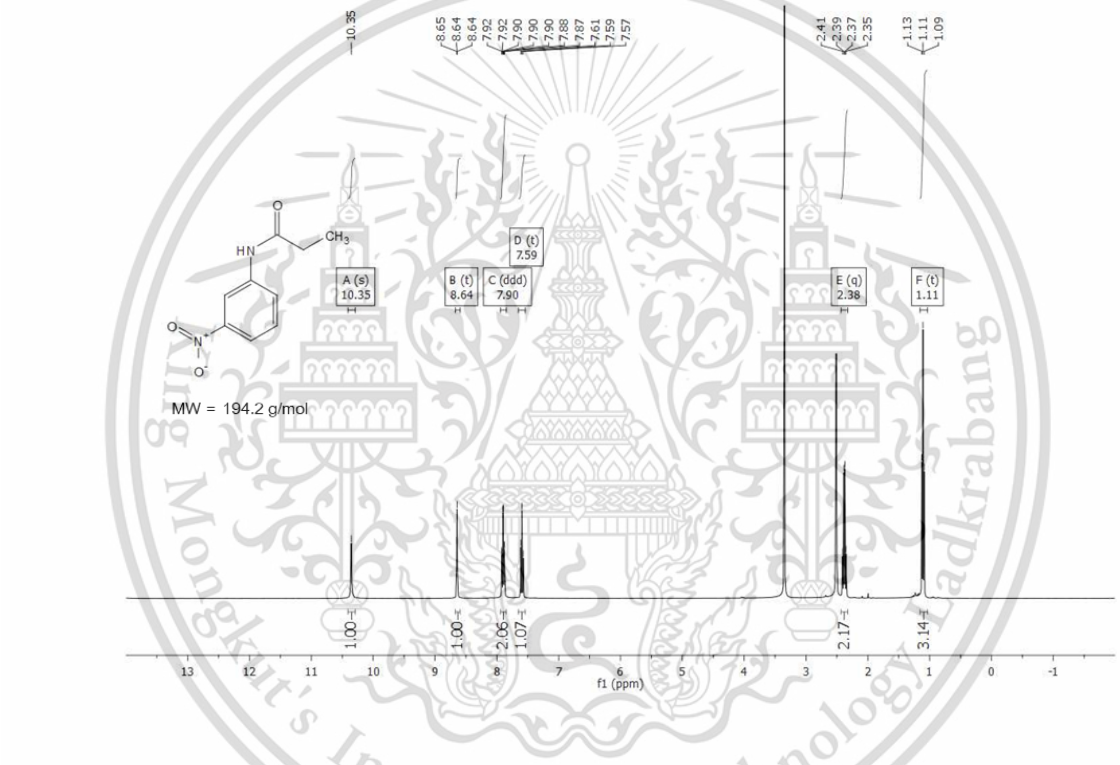

Figure 13. 400 MHz ^{1}H NMR spectrum of N-(3-nitrophenyl) propenamide (compound **5**)

4.2.6 Synthesis of N-(3-aminophenyl)propanamide (6)

A yellow solid was collected to afford the compound **6** (74% yield). ^{1}H NMR (400 MHz, DMSO-d_6) δ 9.52 (s, 1H), 6.92 (s, 1H), 6.89 (t, J = 8.0 Hz, 1H), 6.68 (d, J = 8.0 Hz, 1H), 6.23 (dd, J = 7.9, 1.3 Hz, 1H), 5.01 (s, 2H), 2.26 (q, J = 7.6 Hz, 2H), 1.06 (t, J = 7.6 Hz, 3H).

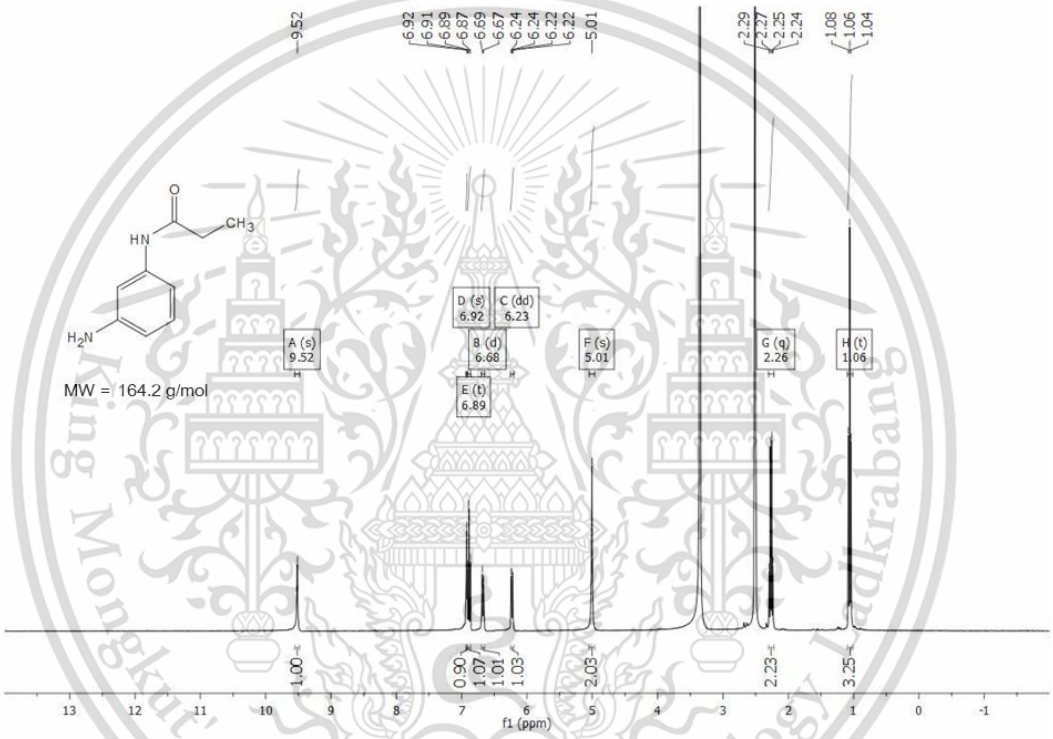

Figure 14. 400 MHz ^{1}H NMR spectrum of N-(3-aminophenyl) propenamide (compound **6**)

4.2.7 Synthesis of N-[3-[(2,5-dichloropyrimidin-4-yl)amino]phenyl]propanamide (7)

A yellow solid was collected to afford the compound **7** (48.9% yield). ^{1}H NMR (400 MHz, DMSO-d_6) δ 9.93 (s, 1H), 9.54 (s, 1H), 8.37 (s, 1H), 7.83 (t, J = 1.9 Hz, 1H), 7.39 (d, J = 8.3 Hz, 1H), 7.30 (t, J = 8.0 Hz, 1H), 7.23 (ddd, J = 8.0, 1.9, 1.2 Hz, 1H), 2.34 (q, J = 7.5 Hz, 2H), 1.09 (t, J = 7.6 Hz, 3H).

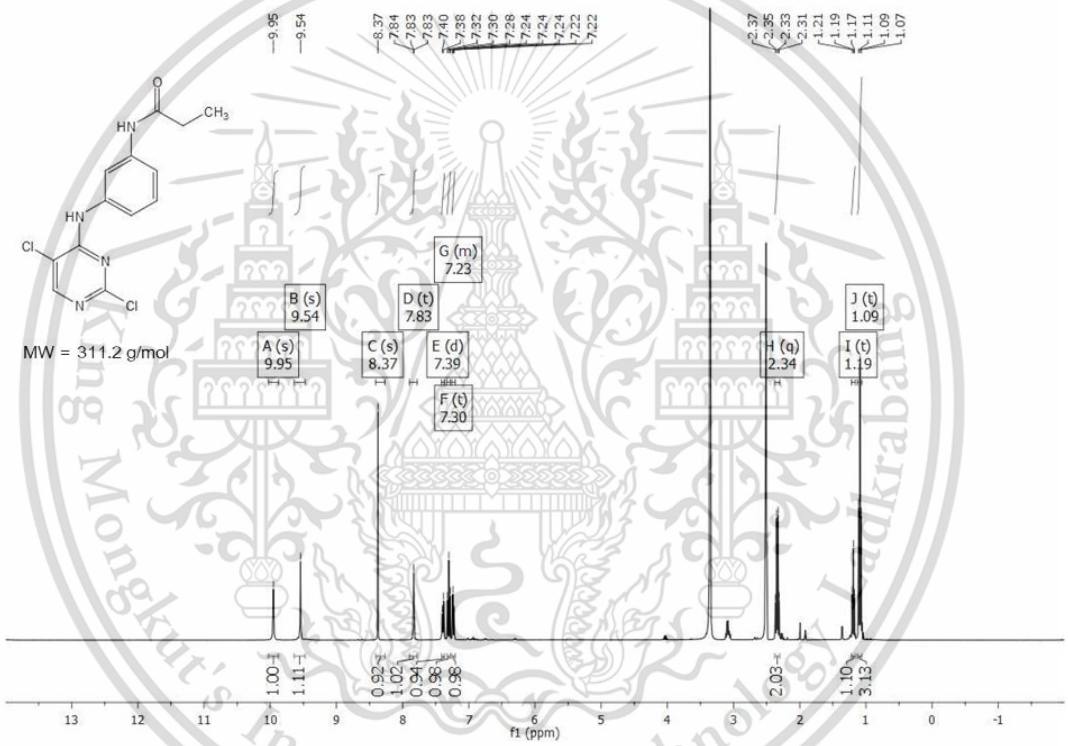

Figure 15. 400 MHz ^{1}H NMR spectrum of N-[3-[(2,5-dichloropyrimidin-4-yl)amino]phenyl]propanamide (compound **7**)

4.2.8 Synthesis of 1-(4-(3-methoxy-4-nitrophenyl)piperazin-1-yl)ethanone (8)

A purple solid was collected to afford the compound **8** (90% yield). ^{1}H NMR (400 MHz, DMSO-d_6) δ 6.53 (dd, J = 5.0, 2.8 Hz, 2H), 6.32 (dd, J = 8.3, 1.9 Hz, 1H), 4.30 (s, 2H), 3.55 (dd, J = 10.6, 6.5 Hz, 4H), 2.97 – 2.83 (m, 4H), 2.08 (s, 1H), 2.03 (s, 3H).

Figure 16. 400 MHz ^{1}H NMR spectrum of 1-(4-(3-methoxy-4-nitrophenyl)piperazin-1-yl)ethanone (compound **8**)

4.2.9 Synthesis of N-[3-[(2-[4-(4-acetylpiperazin-1-yl)-2-methoxyphenyl]amino-5-chloropyrimidin-4-yl)amino]phenyl] propanamide (compound 9)

A light-green solid was collected to afford the product **9** (30% yield). ^{1}H NMR (400 MHz, DMSO-d_6) δ 10.03 (s, 4H), 9.85 (s, 4H), 8.23 (d, J = 1.0 Hz, 3H), 7.89 (d, J = 0.8 Hz, 3H), 7.58 – 7.18 (m, 15H), 6.86 – 6.64 (m, 3H), 6.39 (s, 3H), 3.76 (d, J = 33.6 Hz, 20H), 3.58 (d, J = 11.3 Hz, 43H), 3.14 (d, J = 24.2 Hz, 25H), 2.34 (q, J = 7.5 Hz, 9H), 1.08 (t, J = 7.5 Hz, 13H). ^{13}C NMR (101 MHz, DMSO-d_6) δ 172.58, 168.81, 157.72, 140.07, 137.76, 129.10, 119.73, 116.92, 115.93, 115.92, 107.72, 104.42, 101.01, 56.20, 49.63, 49.63, 49.29, 49.28, 49.27, 45.83, 45.82, 30.00, 21.66, 10.13.

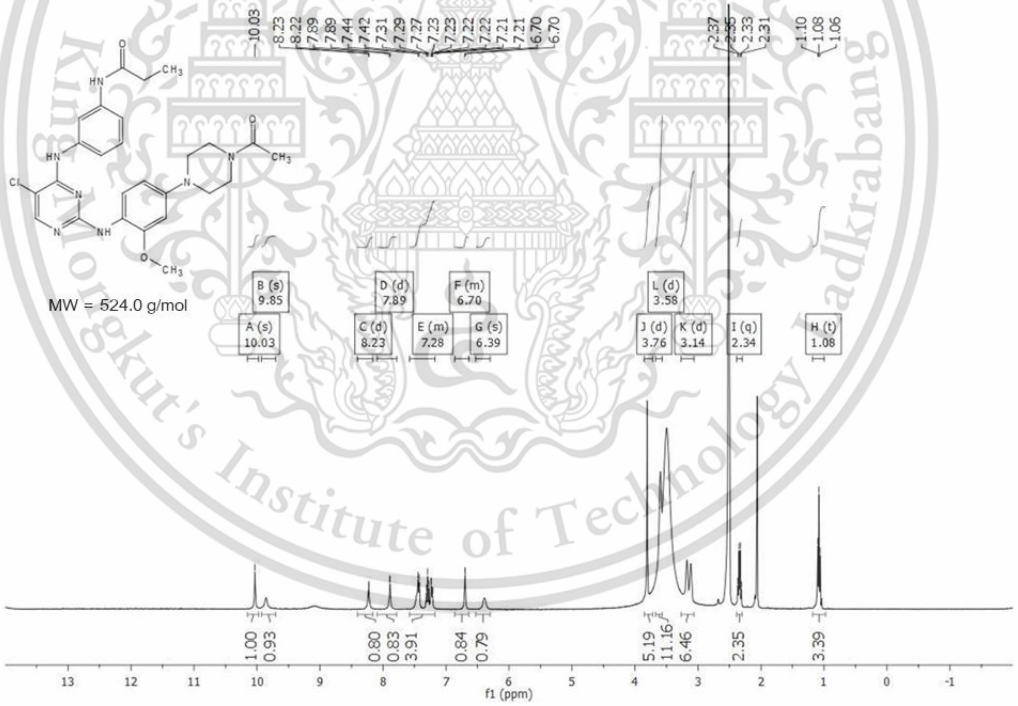

Figure 17. 400 MHz ^{1}H NMR spectrum of N-[3-[(2-[4-(4-acetylpiperazin-1-yl)-2-methoxyphenyl]amino-5-chloropyrimidin-4-yl)amino]phenyl]propenamide (compound **9**)

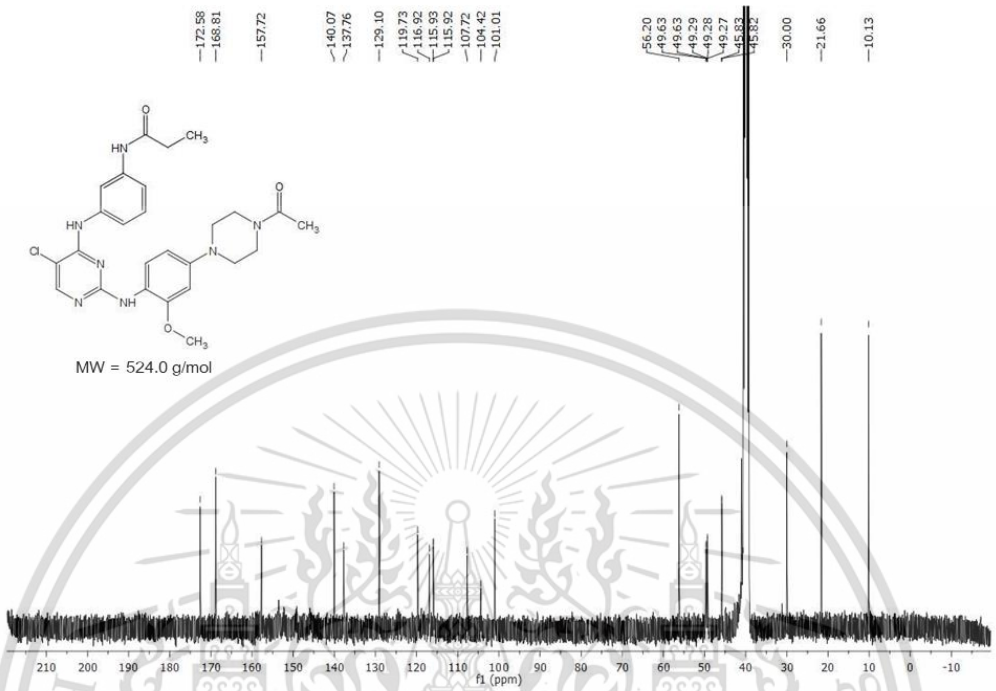

Figure 18. 101 MHz ^{13}C NMR spectrum of N-[3-[(2-[4-(4-acetylpiperazin-1-yl)-2-methoxyphenyl]amino-5-chloropyrimidin-4-yl)amino]phenyl]propenamide (compound **9**)

4.2.10 Exploration of conditions for acid chloride preparation

A series of reactions were undertaken to evaluate the possibility of preparing bespoke acid chlorides. The effect of different reaction conditions on the yield and purity of the acid chlorides were investigated. The effect of using DMF catalyst and the effect of reaction time on the preparation of acryloyl chloride using oxalyl chloride was assessed (Table 1). The presence of the catalyst (DMF) had a large influence on the reaction. Reaction with oxalyl chloride led to the formation of CO, CO_2, HCl. Additionally, it was observed that the double bond of the critical Michael acceptor group is prone to HCl addition, and under these conditions an amount of 3-chloropropionyl chloride was formed.[37]

The course and products from the reactions were evaluated using TLC, H-NMR, IR spectroscopy, HPLC-UV. It should be noted that the latter method proved of little value due to the low stability of the reaction products to high energy ionization conditions (ESI+).

Table 1. The influence of the reaction conditions on the conversion of acrylic acid were screened with oxalyl chloride.

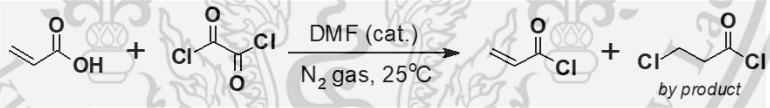

Time (hour)	DMF (equiv.)	$(COCl)_2$ (equiv.)
0.5	✓	3
1	✓	3
2	✓	3
3	✓	3
3	✗	5
4	✓	3
6	✗	5

4.2.10.1 Reagent Spectroscopic Properties (acrylic acid, oxalyl chloride)

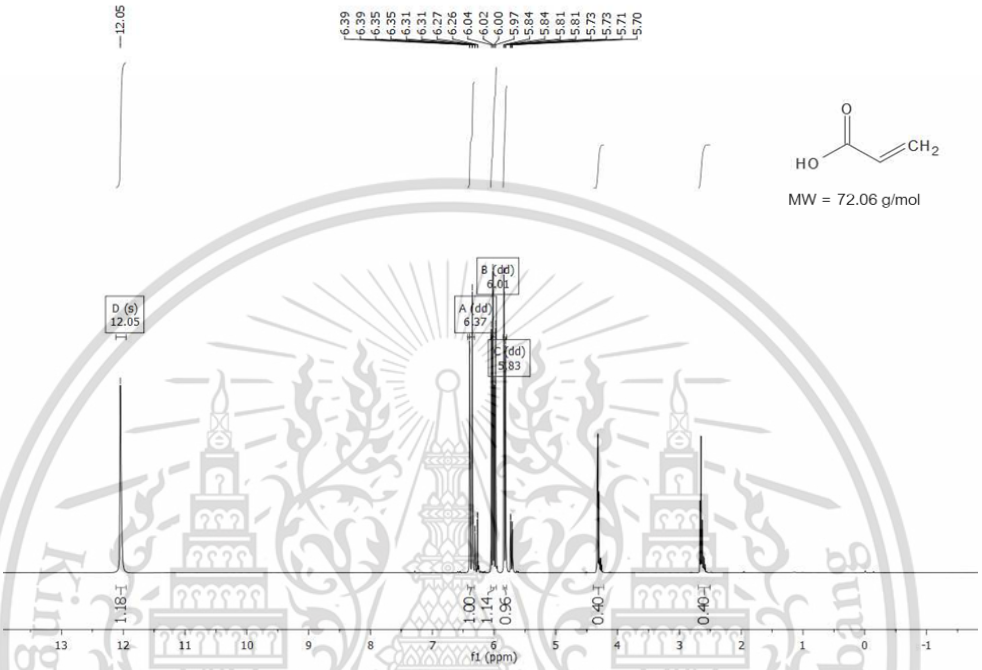

Figure 19. ^{1}H NMR (400 MHz, $CDCl_3$) spectrum of acrylic acid (reactant).

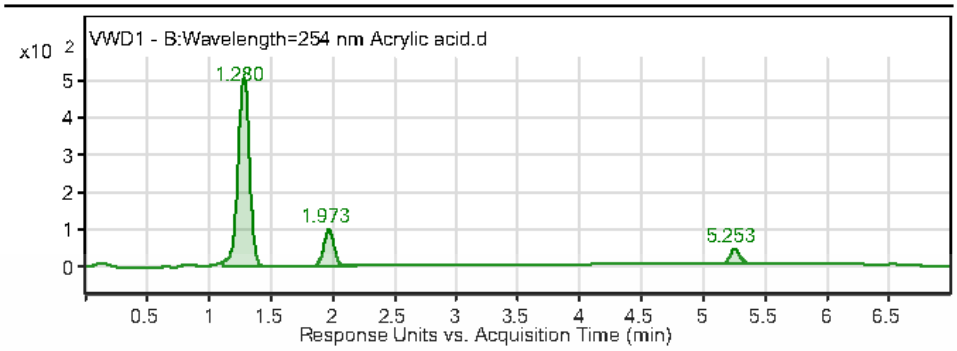

Integration Peak List

Peak	Start	RT	End	Height	Area	Area %
1	1.12	1.28	1.607	510.6	3358.32	100
2	1.829	1.973	2.187	99.42	590.28	17.58
3	5.147	5.253	5.427	39.77	219.1	6.52

Figure 20. Acrylic acid by HPLC chromatogram showing a peak at retention time of 1.280 (100% peak area), 1.973 and 5.253 mins.

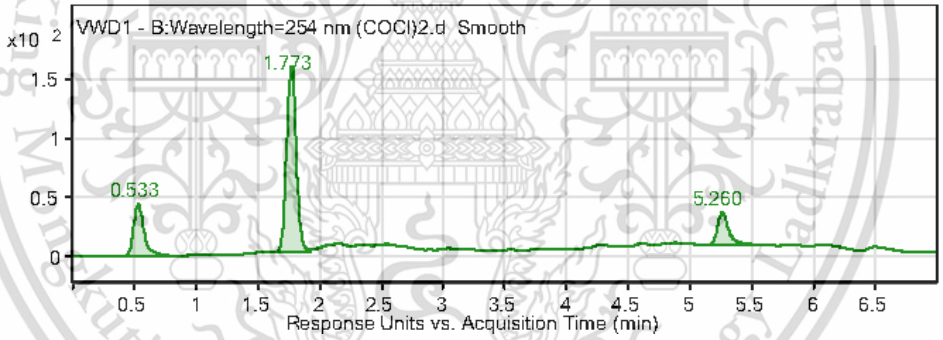

Figure 21. Oxalyl chloride ($(COCl)_2$) by HPLC chromatogram showing a peak at retention time of 0.533, 1.773 (100% peak area) and 5.260 mins.

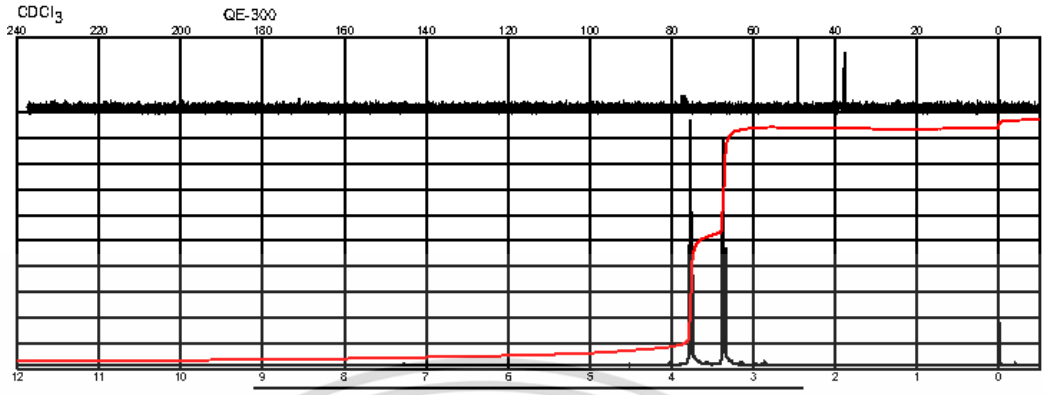

Figure 22. Predicted ^{1}H NMR ($CDCl_3$) of 3-chloropropionyl chloride (from Sigma-Aldrich).

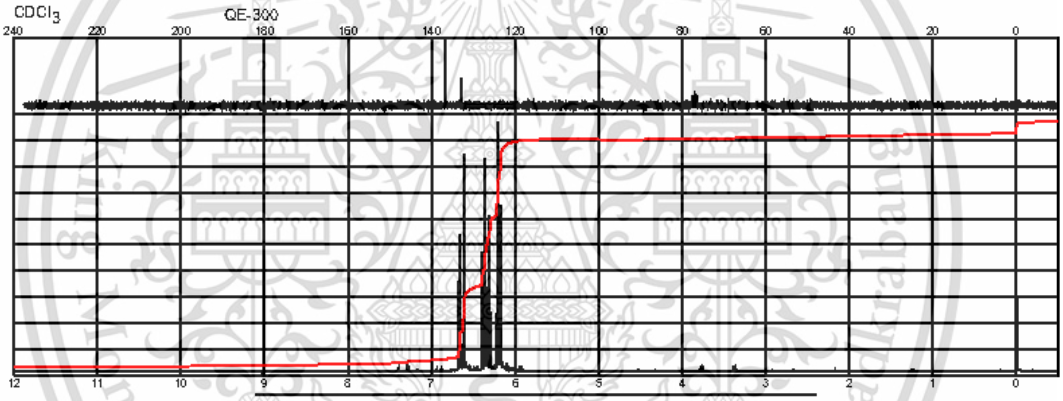

Figure 23. Predicted ^{1}H NMR ($CDCl_3$) of acryloyl chloride (from Sigma-Aldrich).

4.2.10.2 Various time of the reaction

From an analysis of the DMF catalyzed reactions that ranged from 30 minutes to 4 hours, we can see the conversion significantly increased (determined by 1H NMR result Figure 24-28). From, the results at 30 minutes (Figure 24), we can conclude that acrylic acid had not been converted completely. This was due to the intensity of the NMR spectra. Also observed was the presence of impurity from the spectra can show us that the reaction time at 30 minutes is not enough for the conversion. A upfield shift of the acryloyl chloride spectra compared to the reactant (acrylic acid) Figure 19 is apparent. After a prolonged period of time (1–4 hours) the conversion of acrylic acid increases as does the byproduct, determining the %yield of product (the signal at 5.8-6.0 ppm) was decreased from 66% to 37% Figure 25-28. Which can conclude that the optimize reaction should not be longer than 3 hours. The effect of the catalyst (DMF) was further evaluated for experiments.

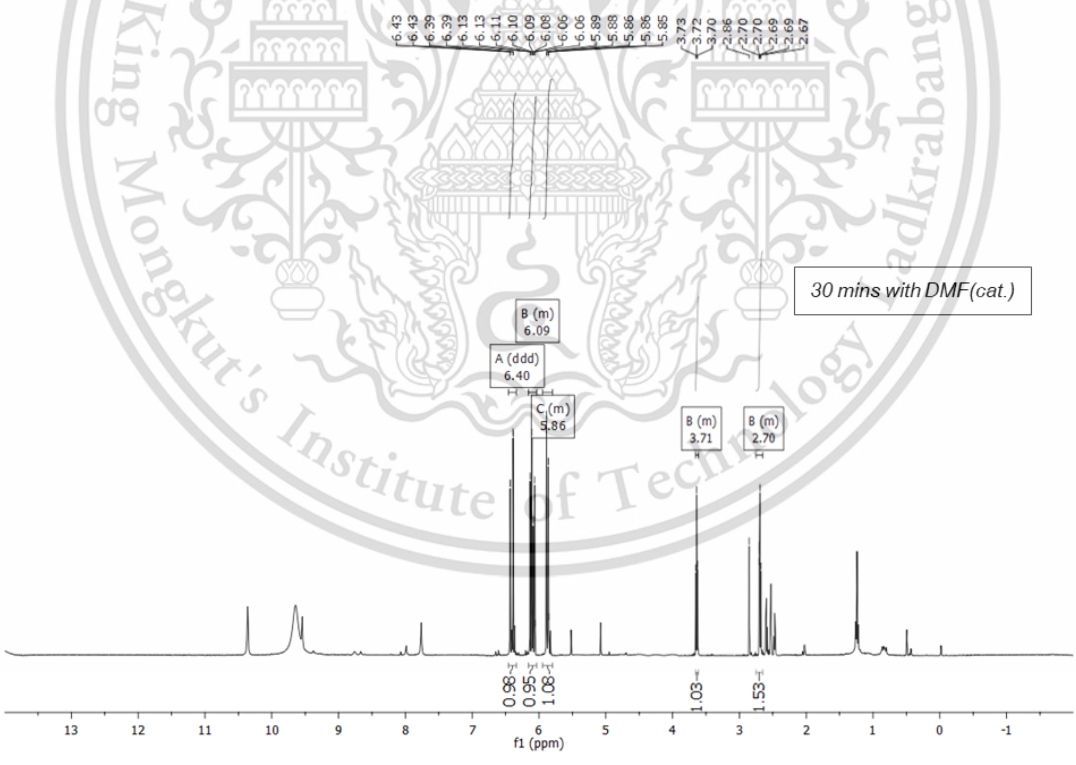

Figure 24. ^{1}H NMR (400 MHz, $CDCl_3$) spectrum of the conversion of acrylic acid to acryloyl chloride with DMF (cat.) at 30 mins. The ratio between product/byproduct is 54:46.

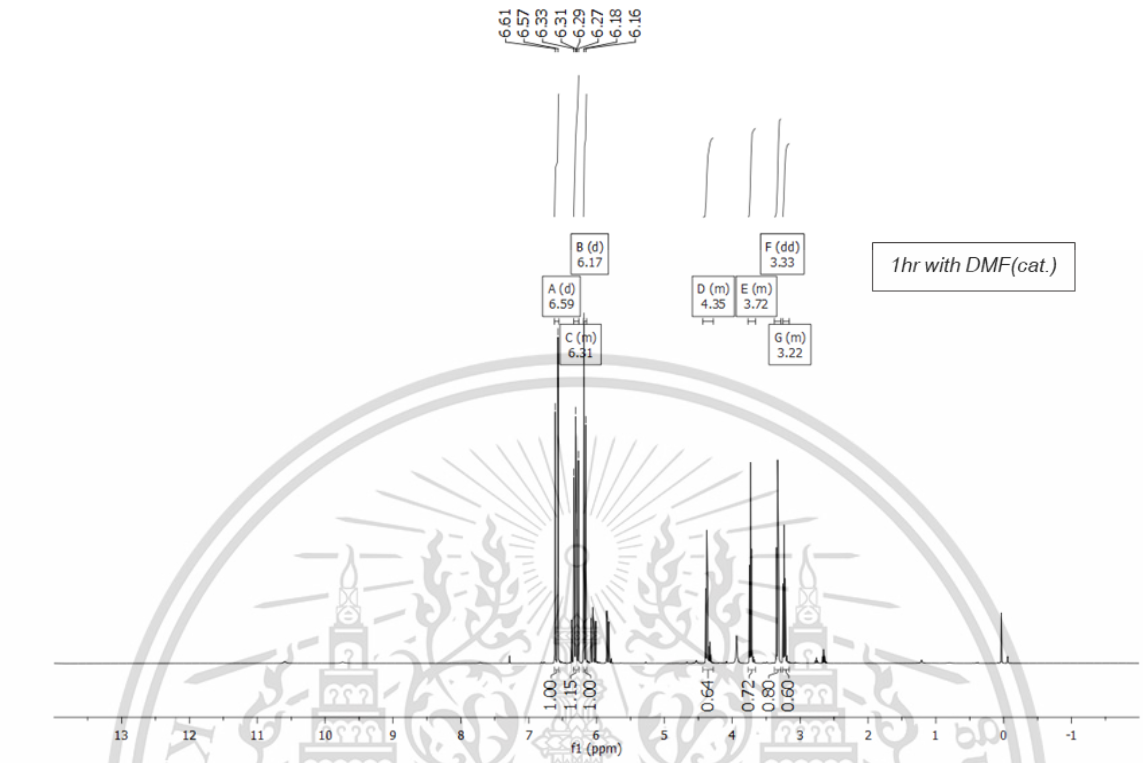

Figure 25. ^{1}H NMR (400 MHz, $CDCl_3$) spectrum of the conversion of acrylic acid to acryloyl chloride with DMF (cat.) at 1 hour. The ratio between product/byproduct is 66:34.

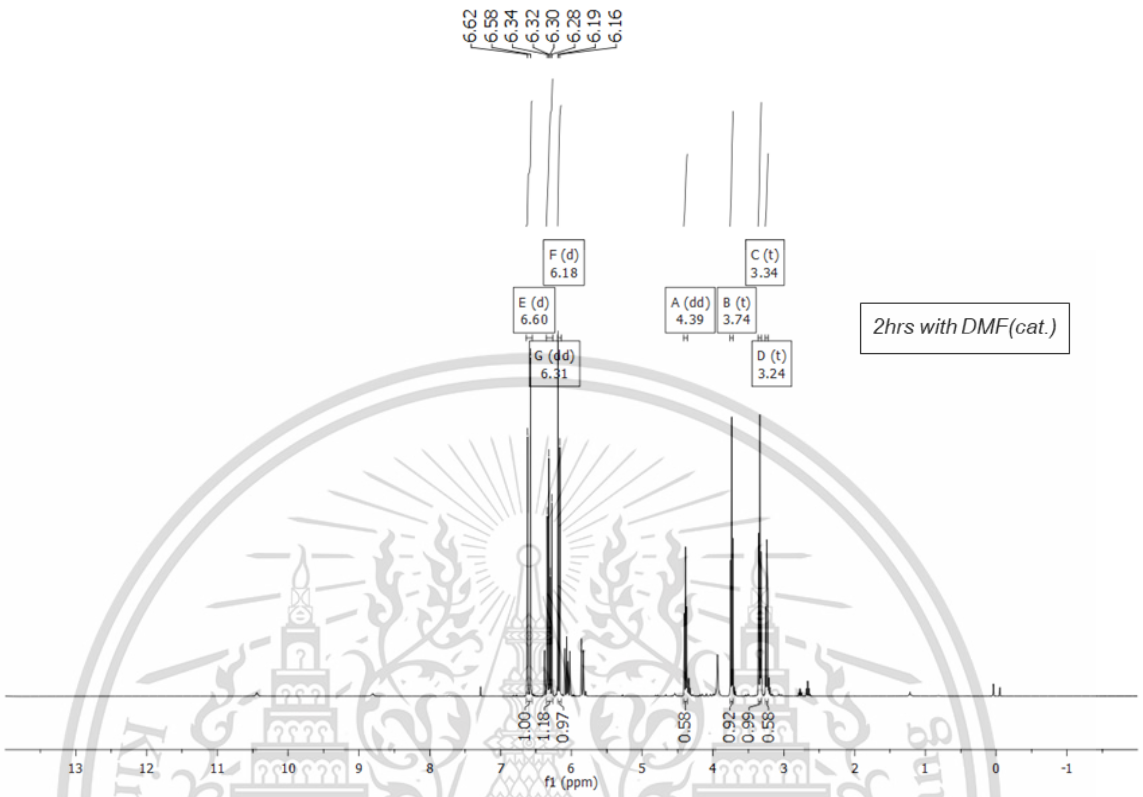

Figure 26. ^{1}H NMR (400 MHz, $CDCl_3$) spectrum of the conversion of acrylic acid to acryloyl chloride with DMF (cat.) at 2 hours. The ratio between product/byproduct is 51:49

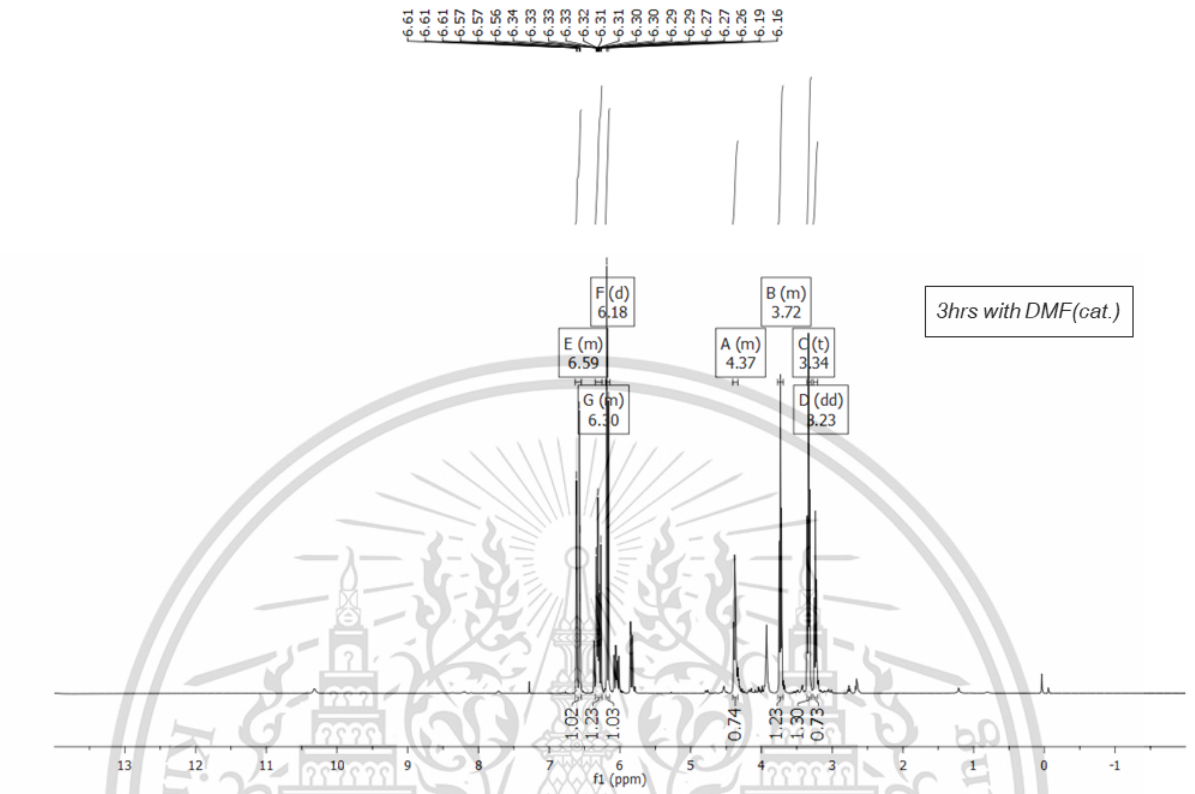

Figure 27. ^{1}H NMR (400 MHz, $CDCl_3$) spectrum of the conversion of acrylic acid to acryloyl chloride with DMF (cat.) at 3 hours. The ratio between product/byproduct is 45:55

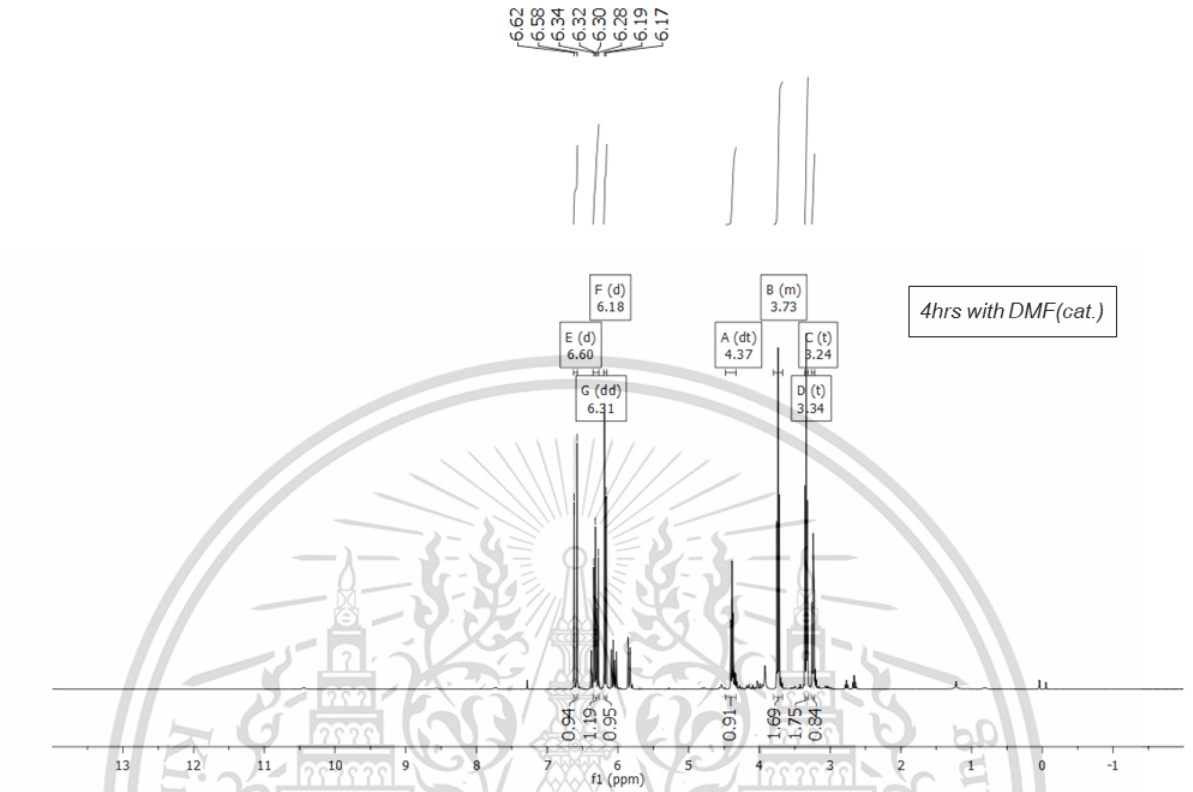

Figure 28. ^{1}H NMR (400 MHz, $CDCl_3$) spectrum of the conversion of acrylic acid to acryloyl chloride with DMF (cat.) at 4 hours. The ratio between product/byproduct is 37:63

4.2.10.3 Observation in the absence of DMF

It was observed that small amounts of DMF were sufficient to enhance the conversion significantly, however the effect it had on the production of impurities were also of concern. The effect of DMF with different reaction time was subsequently evaluated. As with the previous experiment, the reaction products at a time of 30 minutes was not enough for the conversion, even using DMF as a catalyst, which is confirmed by the FTIR spectra (Figure 30a).

Figure 29 and 30 shown the FTIR spectra of the reactant and the product with the various time of the reaction with/without using DMF (cat.) respectively. The intensive peaks at 3070, 2990, 2660 cm^{-1} and 1696 cm^{-1} shown in Figure 29 (left), are due to excitation of stretching vibration mode of hydroxide ions (O-H bonding) and containing the carbonyl stretching vibration mode of carboxylic acid. Whereas, the peaks at 1771 cm^{-}

[1] and 751 cm^{-1} in Figure 29 (right) shown excitation of stretching vibration mode of carbonyl (C=O) and C-Cl of oxalyl chloride. The result from the FTIR spectra can also confirm this hypothesis, comparing the data (Figure 30c, d) in the excitation frequencies of the vibration modes of the reaction that did not use DMF (cat.) at 3 hrs and 6 hrs of reaction shows the broad spectra similar to the reactant (acrylic acid) at 3400 cm^{-1} that means the acrylic acid was not fully converted into acryloyl chloride as well as at 30 mins (Figure30a) even use DMF in the reaction but still shows the broad spectra similar to acrylic acid which mean in the residence time had just slightly converted. On the other hand, the result of the reaction that used DMF (cat.) at 3 hrs (Figure 30b) shows the intensive peaks at 1788 and 669 cm^{-1}, are typically for the stretching vibration modes of carbonyl (C=O) and C-Cl of acid chloride respectively.

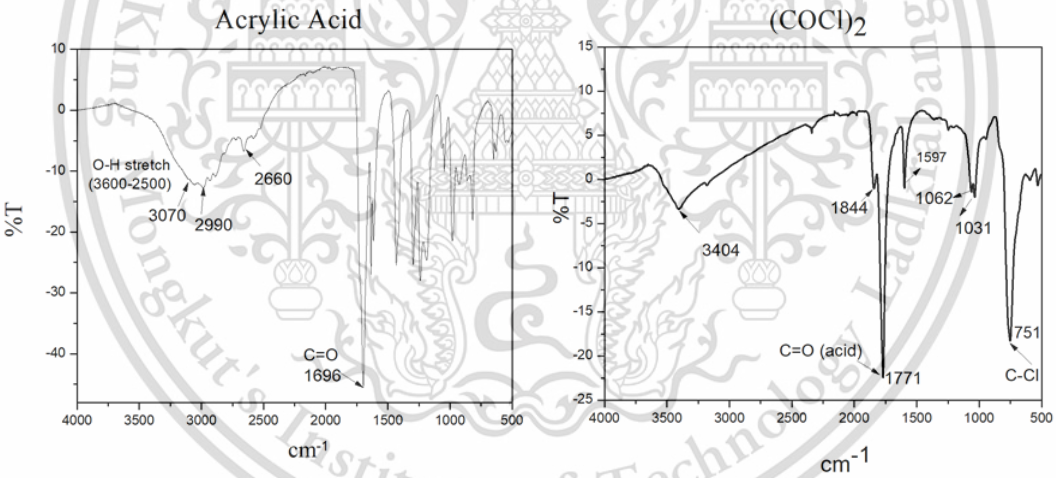

Figure 29. FTIR spectra of the reactant; Acrylic acid (left), Oxalyl chloride ($COCl_2$) (right).

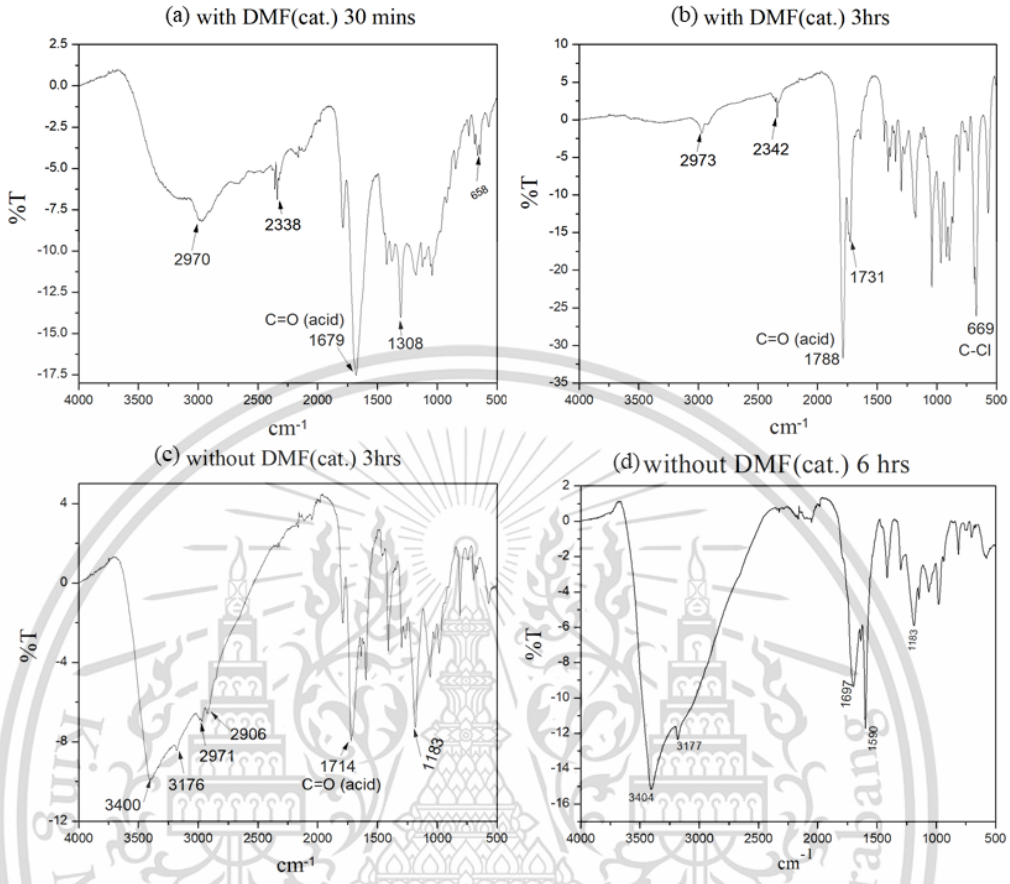

Figure 30. FTIR spectra of the effect of using DMF as catalyst in the conversion. (a) using DMF (cat.) for 30 mins, (b) using DMF (cat.) for 3 hrs, (c) without using DMF (cat.) for 3 hrs and (d) without using DMF (cat.) for 6 hrs.

Based on our earlier discussion of the HPLC spectra, using the DMF in the reaction does lead to the more rapid production of acryloyl chloride compared to conditions where it is not employed as we can see in the HPLC result. As displayed in Figure 31-32 and, using DMF (cat.) for 30 mins and 3 hrs shown the results of the retention time almost the same peak position (3.433 and 3.427 respectively). However, the reaction that did not utilize DMF (cat.) at 3 hrs Figure 33, shown more than one peak and the highest peak at the retention time of 1.667 mins is more slightly close to oxalyl chloride at 1.773 mins. From this it can be assumed that some of this reagent remained in the reaction and did not converted fully. And after running the reaction for 6 hrs without using DMF (cat.) (Figure 34) shown the highest peak at the retention time of 2.193 mins. It might indicate that some

of the acrylic acid has not been fully converted to acryloyl chloride or it could occurred the byproduct (3-chloropropionyl chloride).

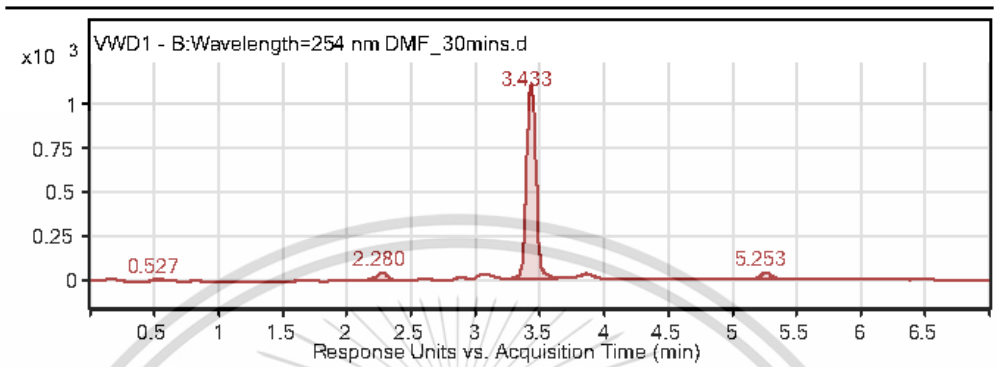

Integration Peak List

Peak	Start	RT	End	Height	Area	Area %
1	0.464	0.527	0.658	14.01	66.1	1.19
2	2.111	2.28	2.37	48.11	280.1	5.02
3	3.313	3.433	3.633	1107.08	5574.26	100
4	5.173	5.253	5.387	38.93	206.82	3.71

Figure 31. The conversion of acrylic acid to acryloyl chloride with DMF (cat.) at 30 mins by HPLC chromatogram showing a peak at retention time of 3.433 mins.

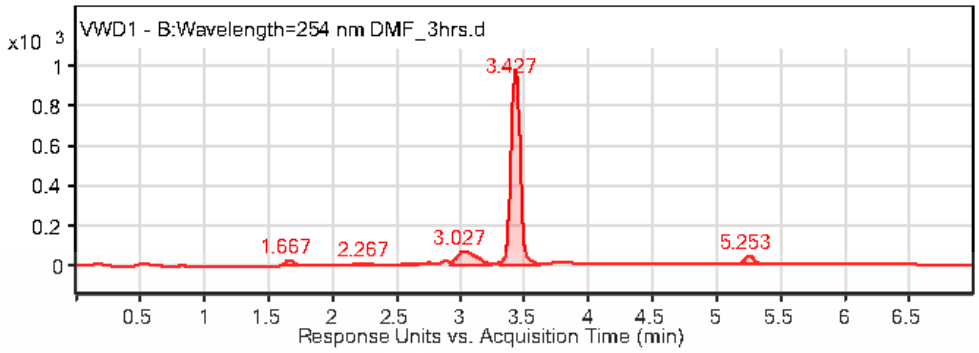

Integration Peak List

Peak	Start	RT	End	Height	Area	Area %
1	1.586	1.667	1.772	31.13	152.05	3.06
2	2.05	2.267	2.387	10.95	107.34	2.16
3	2.407	2.607	2.667	9.63	69.89	1.41
4	2.92	3.027	3.247	68.04	773.22	15.58
5	3.313	3.427	3.62	977.57	4963.55	100
6	5.148	5.253	5.387	39.3	210.1	4.23

Figure 32. The conversion of acrylic acid to acryloyl chloride with DMF (cat.) at 3 hrs by HPLC chromatogram showing a peak at retention time of 3.427 mins.

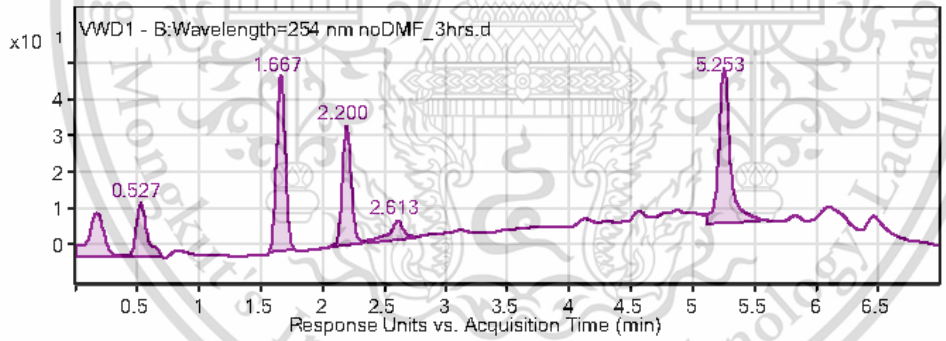

Integration Peak List

Peak	Start	RT	End	Height	Area	Area %
1	0.013	0.173	0.4	11.97	104.01	37.33
2	0.413	0.527	0.706	14.66	88.79	31.87
3	1.573	1.667	1.776	48.38	240.77	86.42
4	2.073	2.2	2.34	32.71	165.65	59.45
5	2.367	2.613	2.76	5.32	48.13	17.27
6	5.113	5.253	5.54	42.67	278.62	100

Figure 33. The conversion of acrylic acid to acryloyl chloride without DMF (cat.) at 3 hrs by HPLC chromatogram showing a peak at retention time of 0.527, 1.667, 2.200, 5.253 mins.

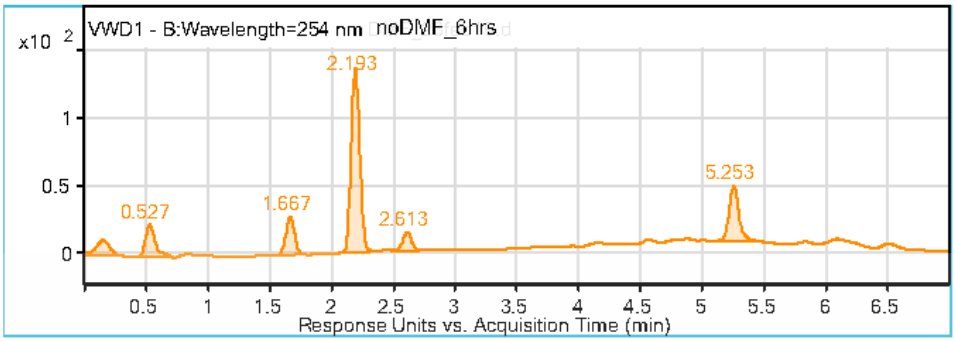

Integration Peak List

Peak	Start	RT	End	Height	Area	Area %
1	0.013	0.153	0.312	11.53	91.96	13.67
2	0.413	0.527	0.693	23.04	123.14	18.3
3	1.567	1.667	1.775	28.24	139.34	20.71
4	2.073	2.193	2.36	136.82	672.79	100
5	2.48	2.613	2.727	13.9	73.46	10.92
6	5.14	5.253	5.42	40.04	223.11	33.16

Figure 34. The conversion of acrylic acid to acryloyl chloride without DMF (cat.) at 6 hrs by HPLC chromatogram showing a peak at retention time of 2.193 mins.

From these results, we can conclude that the ideal reaction should involve the use of DMF, for a time period of hrs to get the most effective conversion of acrylic acid. The %purity calculated from HPLC analysis can confirmed that the reaction should use the DMF. At 30 mins and 3hrs reaction with DMF %purity were 95% and 85.3% respectively. On the other hand, without using DMF at 3 hrs and 6 hrs, the %purity was 49% and 60.7% respectively. From the HPLC analysis we can conclude that using DMF in the reaction could get more purity of product.

4.3 Biological profile

The anti-cancer activity against the A431 cell-line was determined using MTT as well as EGFR inhibitory activity was determining using kinase assay (Table 2). Reported are the concentration required to inhibit cell growth by the half maximal inhibitory concentration (IC_{50}). The cytotoxicity of the compounds against a model human cell line; epidermoid carcinoma (A431) using MTT assay are expressed in the form of an IC_{50}. The solubility of a subset of the most interesting compound (compound **4**) was assessed in terms of their aqueous phosphate buffer (PBS) solubility at pH 7.4 using an equilibrium (thermodynamic) shake-flask technique.

4.3.1 Cytotoxicity at *A431* cell line

All synthesized compounds were assessed in an A431 cell line assay using MTT detection method compared the result to know drugs. The activities are shown the %survival rate results in Figure 35. The result obtained ranged from 0.65 μM to 17.51 μM. Compound **9** show greater potent than compound **4** with an IC_{50} of 1.52 μM while compound **4** show as IC_{50} at 17.51 μM in A431 cell-line. The value of compound **9** was almost equivalent to the known NSCLC anti-cancer drug doxorubicin (IC_{50} = 0.65 μM). Even compound **9** does not has α, β–unsaturated (Michael acceptor) in its structure but it has the same position of 1-(4-(3-Methoxy-4-nitrophenyl)piperazin-1-yl)ethenone as known anti-cancer drug in the maket (Rociletinib). Additionally, this side position might be the resulted in a good potent in A431 cell line. From the result, we can conclude that compound **9** has the most potent observed here while compound **4** has shown relatively poor activity with A431 cell line. In addition, the A431 cell line does not has only EGFR kinase in this cell line which mean compound **9** might has a good potent but it does has poor selectivity at EGFR.

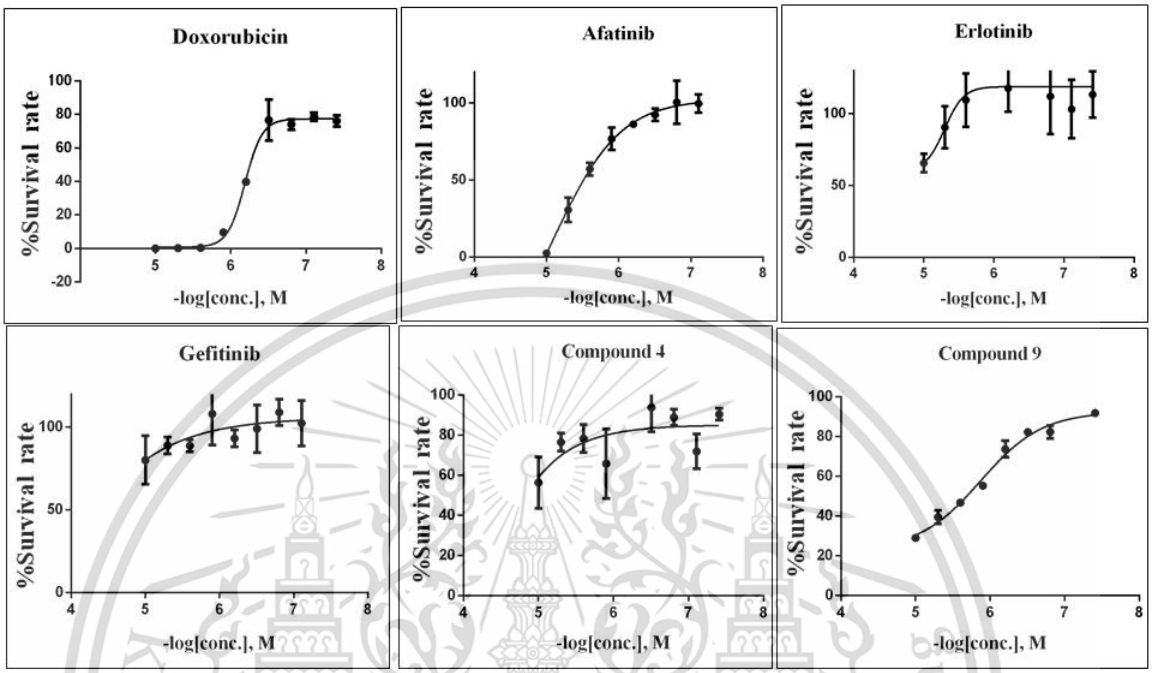

Figure 35. Plot of -log[conc.] vs %survival rate. Compounds **4** and **9** compared with known drugs (Doxorubicin, Afatinib, Erlotinib and Gefitinib) are found to have cytotoxicity in A431 cell at compound **4** = 17.51, compound **9** = 1.52, 0.65, 4.58, 5.04, and 4.06 μM respectively. Data fitting was performed using Prism 6.0 GraphPad Software Inc., (San Diego, CA, USA).

4.3.2 EGFR assay

The biological testing of EGFR inhibitory activity was determined by using kinase inhibition assay. The result shows the compound **4** exhibited good EGFR inhibitory activity (IC_{50} = 1.29 nM), and more potent than Erlotinib and Afatinib with IC_{50}s of 5.29 nM and 0.11 nM, respectively (Figure 36). Compound **4** shown good activity in affinity of EGFR biological assay and also indicated good affect in A431 cell line sililar to drugs cancer on the market. The reactive acrylamides may represent a compromise with respect to covalently target a rare cysteine (Cys797) in EGFR at the lip of the ATP-binding site. This confirms it has cellular selectivity activity with EGFR however, given it is lower than that

obtained by Afatinib, further testing on alterative cell lines, and additional structural modification should be incorporated to improve the lead series further. [14]

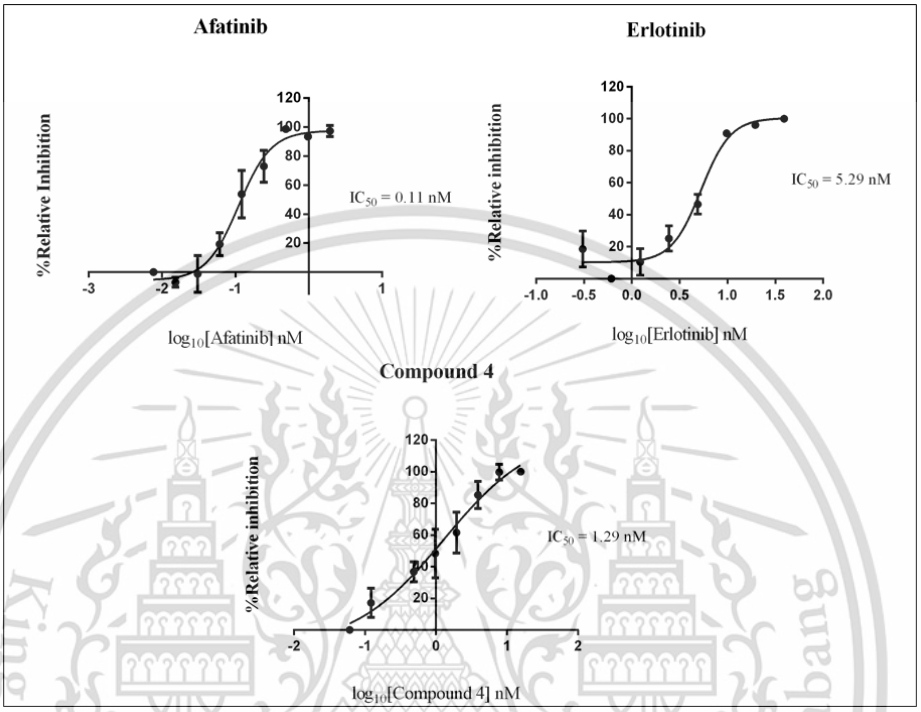

Figure 36. Plot of log[conc.] vs %relative inhibition. Compounds **4** compared with known drugs (Afatinib, Erlotinib) are found to have EGFR kinase activity at 1.29 nM while Afatinib has IC_{50} at 0.11 nM and Erlotinib has IC_{50} at 5.29 nM.

Table 2. Summary of molecular weight, clogP, solubility and activity of compound **4** and **9** compared with known drugs for A431 cell line and EGFR inhibition.

ID	Structure	clogP[a]	MWT[a]	IC_{50} (nM) EGFR	IC_{50} (μM) A431	Solubility pH 7.4 μg/mL
4	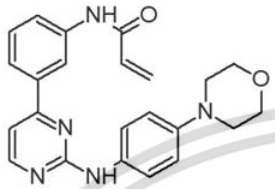	4.1	401.9	1.29	17.51	1.13
9	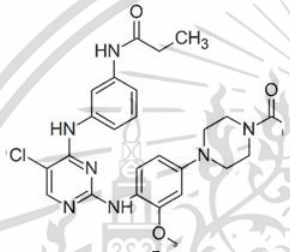	3.8	524.0	-	1.52	-
Afatinib	-	3.4	485.9	0.11	4.58	-
Erlotinib	-	3.2	393.4	5.29	5.04	-
Gefitinib	-	3.8	446.9	-	4.06	-
Doxorubicin	-	0.5	543.5	-	0.65	-

[a] MWT and clogP was calculated using Jchem Version 18.11.0.301

Chapter 5

Conclusion and Suggestion

The primary of this study was to study the route of synthesis with the new and potent covalent inhibitor for lung cancer. With the novel compounds based on pyrimidine scaffold synthesized to act as covalent inhibitors of EGFR as well as determining more extensively the cytotoxic potential at further cell-line compared with known drugs and the non-covalent compound (compound **9**) also.

The most potent compound is compound **9** with A431 cell-line activity with an IC_{50} value 1.52 μM compared with compound **4** with the result is 17.51 μM in A431 cell-line. And This compound **9** was almost equivalent to the known NSCLC anti-cancer drug doxorubicin (IC_{50} = 0.65 μM). From the result, the A431 cell line does not has only overexpressed EGFR in this cell line which mean compound **9** might has a good potent and activity but it does has poor selectivity at EGFR cell line. In addition, we reported our efforts to synthesize and evaluate phenylamino-pyrimidine based compound for its potential to exhibit an anti-EGFR kinase activity at the nanomolar range, compound **4** has been prepared in moderate yield and the compounds potency at EGFR (IC_{50} = 1.29 nM) has been shown to be good potent inhibition at EGFR than Erlotinib (IC_{50} = 5.29 μM). But compound **4** has lower potency than Afatinib. In summary, even compound **4** has a poor activity at A431 cell line suggesting this compound do not display non-specific cytotoxicity but it has a very good activity in EGFR assay which means that compound **4** has a good selectivity compared with known drugs.

The screening of oxalyl chloride mediated synthesis of acid chloride by prolonging the reaction time with DMF as catalyst, excellent conversion towards acryloyl chloride was achieved with the use of DMF in 1-2 hours. At these times of reaction should gave the full conversion of acrylic acid. Whereas, the complication of conversion of acrylic acid, its rapid and highly exothermic synthesis which is extremely difficult to control the reaction system. Problems that concern the purity of acryloyl chloride and the hazardous nature of the chlorinating reagents and the byproducts. The next step in the processes is to prepare

new analogs lying outside of the known patent and publication space with a view to obtaining improved potency, selectivity, and good physical properties. Additional effort will be spent on the use of acid chloride reagents to more rapidly expand the SAR of the series and to improve the yield.

Reference

1. Bostrom, J., et al., *Expanding the medicinal chemistry synthetic toolbox.* Nat Rev Drug Discov, 2018. **17**(10): p. 709-727.

2. Siegel, R.L., K.D. Miller, and A. Jemal, *Cancer statistics, 2017.* CA Cancer J Clin., 2017. **67**(1): p. 7-30.

3. Jemal A, B.F., Center MM, Ferlay J, Ward E, Forman D, *Global cancer statistics.* CA Cancer J Clin, 2011. **61**: p. 69–90.

4. Siegel, R., et al., *Cancer statistics, 2014.* CA: a cancer journal for clinicians, 2014. **64**(1): p. 9-29.

5. Sankaranarayanan, R., K. Ramadas, and Y.-l. Qiao, *Managing the changing burden of cancer in Asia.* BMC medicine, 2014. **12**(1): p. 3.

6. Lynch, T.J., et al., *Activating mutations in the epidermal growth factor receptor underlying responsiveness of non–small-cell lung cancer to gefitinib.* New England Journal of Medicine, 2004. **350**(21): p. 2129-2139.

7. Wang, X., et al., *Next-generation EGFR/HER tyrosine kinase inhibitors for the treatment of patients with non-small-cell lung cancer harboring EGFR mutations: a review of the evidence.* OncoTargets Ther, 2016. **9**: p. 5461.

8. Midha, A., S. Dearden, and R. McCormack, *EGFR mutation incidence in non-small-cell lung cancer of adenocarcinoma histology: a systematic review and global map by ethnicity (mutMapII).* Am J Cancer Res, 2015. **5**(9): p. 2892.

9. Midha, A., S. Dearden, and R. McCormack, *EGFR mutation incidence in non-small-cell lung cancer of adenocarcinoma histology: a systematic review and global map by ethnicity (mutMapII).* American Journal of Cancer Research, 2015. **5**(9): p. 2892-2911.

10. Chalkidou, K., et al., *Evidence-informed frameworks for cost-effective cancer care and prevention in low, middle, and high-income countries.* The lancet oncology, 2014. **15**(3): p. 119-131.

11. Zhang, J., P.L. Yang, and N.S. Gray, *Targeting cancer with small molecule kinase inhibitors.* Nature reviews cancer, 2009. **9**(1): p. 28.

12. Sever, R. and J.S. Brugge, *Signal transduction in cancer.* Cold Spring Harbor perspectives in medicine, 2015. **5**(4): p. a006098.

13. Ghafoor, Q., et al., *Epidermal Growth Factor Receptor (EGFR) Kinase Inhibitors and Non-Small Cell Lung Cancer (NSCLC)–Advances in Molecular Diagnostic Techniques to Facilitate Targeted Therapy.* Pathology & Oncology Research, 2018. **24**(4): p. 723-731.

14. Engel, J., J. Lategahn, and D. Rauh, *Hope and disappointment: covalent inhibitors to overcome drug resistance in non-small cell lung cancer*. 2015, ACS Publications.

15. Zhou, W., et al., *Novel mutant-selective EGFR kinase inhibitors against EGFR T790M.* Nature, 2009. **462**(7276): p. 1070-4.

16. Hirsh, V., *Next-Generation Covalent Irreversible Kinase Inhibitors in NSCLC: Focus on Afatinib.* BioDrugs : clinical immunotherapeutics, biopharmaceuticals and gene therapy, 2015. **29**(3): p. 167-183.

17. Hoang, T. and J.H. Schiller, *Advanced NSCLC: from cytotoxic systemic chemotherapy to molecularly targeted therapy.* Expert review of anticancer therapy, 2002. **2**(4): p. 393-401.

18. Ansari, J., et al., *Role of tyrosine kinase inhibitors in lung cancer.* Anti-Cancer Agents in Medicinal Chemistry (Formerly Current Medicinal Chemistry-Anti-Cancer Agents), 2009. **9**(5): p. 569-575.

19. Liu, Q., et al., *Developing irreversible inhibitors of the protein kinase cysteinome.* Chemistry & biology, 2013. **20**(2): p. 146-159.

20. Traxler, P. and P. Furet, *Strategies toward the design of novel and selective protein tyrosine kinase inhibitors.* Pharmacol Ther, 1999. **82**(2-3): p. 195-206.

21. Sunpaweravong, P., *Tyrosine kinase receptor inhibitor as a molecularly targeted therapy for solid tumors.* Songklanagarind Medical Journal, 2006. **24**(1): p. 43-52.

22. Du, Z. and C.M. Lovly, *Mechanisms of receptor tyrosine kinase activation in cancer.* Molecular cancer, 2018. **17**(1): p. 58.

23. Heldin, C.-H., *Dimerization of cell surface receptors in signal transduction.* Cell, 1995. **80**(2): p. 213-223.

24. da Cunha Santos, G., F.A. Shepherd, and M.S. Tsao, *EGFR mutations and lung cancer.* Annual Review of Pathology: Mechanisms of Disease, 2011. **6**: p. 49-69.

25. Thomas, A., A. Rajan, and G. Giaccone, *Tyrosine kinase inhibitors in lung cancer.* Hematology/Oncology Clinics, 2012. **26**(3): p. 589-605.

26. Roengvoraphoj, M., et al., *Epidermal growth factor receptor tyrosine kinase inhibitors as initial therapy for non-small cell lung cancer: focus on epidermal*

growth factor receptor mutation testing and mutation-positive patients. Cancer treatment reviews, 2013. **39**(8): p. 839-850.

27. De Cesco, S., Kurian, J., Dufresne, C., Mittermaier, A.K. and Moitessier, N., *Covalent inhibitors design and discovery.* . Eur J Med Chem, 2017. **138**: p. 96-114.

28. Wang L, Z.J., Yao Y, Wang C, Zhang J, Shu X, Sun X, Li Y, Liu K, Yuan H, Ma X. , *Covalent binding design strategy: A prospective method for discovery of potent targeted anticancer agents.* Eur J Med Chem, 2017. **142**: p. 493-505.

29. Singh, J., Petter, R.C., Baillie, T.A. and Whitty, A., *The resurgence of covalent drugs.* Nature reviews Drug discovery, 2011. **10**(4): p. 307.

30. Bauer, R.A., *Covalent inhibitors in drug discovery: from accidental discoveries to avoided liabilities and designed therapies.* Drug Discov Today, 2015. **20**(9): p. 1061-1073.

31. Cheng, H., et al., *Discovery of 1-{(3R,4R)-3-[({5-Chloro-2-[(1-methyl-1H-pyrazol-4-yl)amino]-7H-pyrrolo[2,3-d]pyr imidin-4-yl}oxy)methyl]-4-methoxypyrrolidin-1-yl}prop-2-en-1-one (PF-06459988), a Potent, WT Sparing, Irreversible Inhibitor of T790M-Containing EGFR Mutants.* J Med Chem, 2016. **59**(5): p. 2005-24.

32. Kalgutkar, A.S. and D.K. Dalvie, *Drug discovery for a new generation of covalent drugs.* Expert opinion on drug discovery, 2012. **7**(7): p. 561-581.

33. Anderson, A.C., *The process of structure-based drug design.* Chemistry & biology, 2003. **10**(9): p. 787-797.

34. Roughley, S.D. and A.M. Jordan, *The Medicinal Chemist's Toolbox: An Analysis of Reactions Used in the Pursuit of Drug Candidates.* J. Med. Chem., 2011. **54**(10): p. 3451-3479.

35. Jordan, A.M. and S.D. Roughley, *Drug discovery chemistry: a primer for the non-specialist.* Drug Discovery Today, 2009. **14**(15): p. 731-744.

36. Ward, R.A., et al., *Structure- and reactivity-based development of covalent inhibitors of the activating and gatekeeper mutant forms of the epidermal growth factor receptor (EGFR).* J Med Chem, 2013. **56**(17): p. 7025-48.

37. Movsisyan M, H.T., Dams R, Stevens CV., *Safe, Selective, and High-Yielding Synthesis of Acryloyl Chloride in a Continuous-Flow System.* ChemSusChem, 2016. **9**: p. 1945-1952.

38. Ding, L., et al., *Linear, Y-shaped, and H-shaped amphiphilic azobenzene copolymers: Facile synthesis and topological effect on self-assembly and photoresponsive property.* Reactive and Functional Polymers, 2017. **121**: p. 15-22.

39. Wimmer, L., et al., *Developing piperine towards TRPV1 and GABA A receptor ligands–synthesis of piperine analogs via Heck-coupling of conjugated dienes.* Organic & biomolecular chemistry, 2015. **13**(4): p. 990-994.

40. Phuangsawai, O., et al., *Evaluation of the anti-malarial activity and cytotoxicity of 2,4-diamino-pyrimidine-based kinase inhibitors.* Eur J Med Chem, 2016. **124**: p. 896-905.

41. Sangpheak, K., et al., *Computational screening of chalcones acting against topoisomerase IIα and their cytotoxicity towards cancer cell lines.* J Enzyme Inhib Med Chem, 2019. **34**(1): p. 134-143.

APPENDIX

Poster Presentations

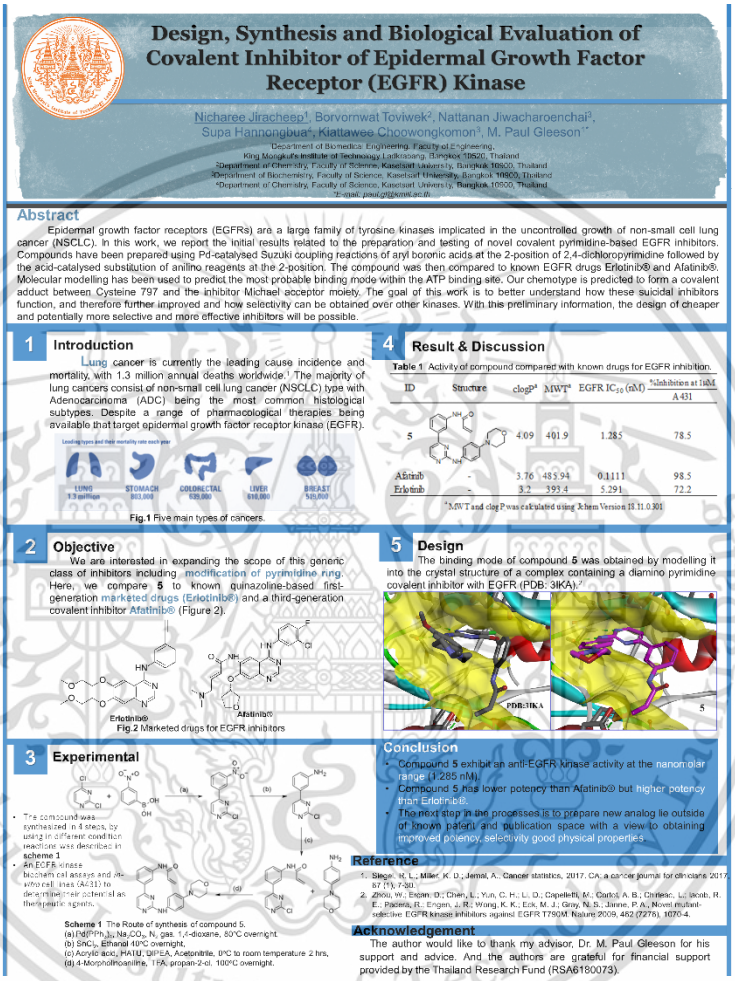

Design, Synthesis and Biological Evaluation of Covalent Inhibitor of Epidermal Growth Factor Receptor (EGFR) Kinase

Nicharee Jiracheep[1], Borvornwat Toviwek[2], Nattanan Jiwacharoenchai[3], Supa Hannongbua[4], Klattawee Choowongkomon[5], M. Paul Gleeson[1*]
[1]Department of Biomedical Engineering, Faculty of Engineering, King Mongkut's Institute of Technology Ladkrabang, Bangkok 10520, Thailand
[2]Department of Chemistry, Faculty of Science, Kasetsart University, Bangkok 10900, Thailand
[3]Department of Biochemistry, Faculty of Science, Kasetsart University, Bangkok 10900, Thailand
[4]Department of Chemistry, Faculty of Science, Kasetsart University, Bangkok 10900, Thailand
[5]E-mail: paul.gl@kmitl.ac.th

Abstract

Epidermal growth factor receptors (EGFRs) are a large family of tyrosine kinases implicated in the uncontrolled growth of non-small cell lung cancer (NSCLC). In this work, we report the initial results related to the preparation and testing of novel covalent pyrimidine-based EGFR inhibitors. Compounds have been prepared using Pd-catalysed Suzuki coupling reactions of aryl boronic acids at the 2-position of 2,4-dichloropyrimidine followed by the acid-catalysed substitution of anilino reagents at the 2-position. The compound was then compared to known EGFR drugs Erlotinib® and Afatinib®. Molecular modelling has been used to predict the most probable binding mode within the ATP binding site. Our chemotype is predicted to form a covalent adduct between Cysteine 797 and the inhibitor Michael acceptor moiety. The goal of this work is to better understand how these suicidal inhibitors function, and therefore further improved and how selectivity can be obtained over other kinases. With this preliminary information, the design of cheaper and potentially more selective and more effective inhibitors will be possible.

1 Introduction

Lung cancer is currently the leading cause incidence and mortality, with 1.3 million annual deaths worldwide.[1] The majority of lung cancers consist of non-small cell lung cancer (NSCLC) type with Adenocarcinoma (ADC) being the most common histological subtypes. Despite a range of pharmacological therapies being available that target epidermal growth factor receptor kinase (EGFR).

Fig.1 Five main types of cancers.

2 Objective

We are interested in expanding the scope of this generic class of inhibitors including modification of pyrimidine ring. Here, we compare **5** to known quinazoline-based first-generation marketed drugs (Erlotinib®) and a third-generation covalent inhibitor Afatinib® (Figure 2).

Fig.2 Marketed drugs for EGFR inhibitors

3 Experimental

- The compound was synthesized in 4 steps, by using in different condition reactions was described in scheme 1
- An EGFR kinase biochemical assays and A-549 cell lines (A431) to determine their potential as therapeutic agents.

Scheme 1 The Route of synthesis of compound 5.
(a) $Pd(PPh_3)_4$, Na_2CO_3, N_2 gas, 1,4-dioxane, 80°C overnight.
(b) $SnCl_2$, Ethanol 40°C overnight.
(c) Acryloyl chloride, PhH3, DIPEA, Acetonitrile, 0°C to room temperature 2 hrs.
(d) 4-Morpholinoaniline, TFA, propan-2-ol, 100°C overnight.

4 Result & Discussion

Table 1 Activity of compound compared with known drugs for EGFR inhibition.

ID	Structure	clogP[a]	MWT[a]	EGFR IC_{50} (nM)	%Inhibition at 1uM A 431
5		4.09	401.9	1.285	78.5
Afatinib	-	3.76	485.94	0.1111	98.5
Erlotinib	-	3.2	393.4	5.291	72.2

[a]MWT and clogP was calculated using Chem Version 18.11.0.301

5 Design

The binding mode of compound **5** was obtained by modelling it into the crystal structure of a complex containing a diamino pyrimidine covalent inhibitor with EGFR (PDB: 3IKA).[2]

Conclusion

- Compound **5** exhibit an anti-EGFR kinase activity at the nanomolar range (1.285 nM).
- Compound **5** has lower potency than Afatinib® but higher potency than Erlotinib®.
- The next step in the processes is to prepare new analog lie outside of known patent and publication space with a view to obtaining improved potency, selectivity good physical properties.

Reference

1. Siegel, R. L., Miller, K. D., Jemal, A. Cancer statistics, 2017. CA: a cancer journal for clinicians 2017, 67 (1), 7-30.
2. Zhou, W., Ercan, D., Chen, L., Yun, C. H., Li, D., Capelletti, M., Cortot, A. B., Chirieac, L., Iacob, R. E., Padera, R., Engen, J. R., Wong, K. K., Eck, M. J., Gray, N. S., Jänne, P. A., Novel mutant-selective EGFR kinase inhibitors against EGFR T790M. Nature 2009, 462 (7276), 1070-4.

Acknowledgement

The author would like to thank my advisor, Dr. M. Paul Gleeson for his support and advice. And the authors are grateful for financial support provided by the Thailand Research Fund (RSA6180073).

Author Biography

NAME : Ms. NICHAREE JIRACHEEP

BIRTH DATE : May 19, 1994

BIRTHPLACE : Phitsanulok, Thailand

EDUCATION : 2016-2012 Bachelor of Science (Chemistry)
Major: Industrial Chemistry (Minor: Material Science),
King Mongkut's Institute of Technology Ladkrabang

E-MAIL : njiracheep@gmail.com